



THESIS APPROVAL
GRADUATE SCHOOL, KASETSART UNIVERSITY

Master of Science (Food Science)

DEGREE

Food Science

FIELD

Food Science and Technology

DEPARTMENT

TITLE: Formation of Solid Foam Structure and Oil Absorption of Fried Snacks
from Rice Flour Composites

NAME: Miss Sasikarn Kithikorn

THIS THESIS HAS BEEN ACCEPTED BY

THESIS ADVISOR

(Associate Professor Parichat Hongsprabhas, Ph.D.)

THESIS CO-ADVISOR

(Assistant Professor Masubon Thongngam, Ph.D.)

DEPARTMENT HEAD

(Assistant Professor Tanaboon Sajjaanantakul, Ph.D.)

APPROVED BY THE GRADUATE SCHOOL ON _____

DEAN

(Associate Professor Gunjana Theeragool, D.Agr.)

THESIS

FORMATION OF SOLID FOAM STRUCTURE AND
OIL ABSORPTION OF FRIED SNACKS FROM
RICE FLOUR COMPOSITES

SASIKARN KITHIKORN

A Thesis Submitted in Partial Fulfillment of
the Requirements for the Degree of
Master of Science (Food Science)
Graduate School, Kasetsart University

2009

Sasikarn Kithikorn 2009: Formation of Solid Foam Structure and Oil Absorption of Fried Snacks from Rice Flour Composites. Master of Science (Food Science), Major Field: Food Science, Department of Food Science and Technology. Thesis Advisor: Associate Professor Parichat Hongsprabhas, Ph.D. 82 pages.

This study investigated the influences of flour composition, protein content and ratios of rice flour to waxy rice flour (at 1.0:0.0, 0.9:0.1, 0.8:0.2 and 0.7:0.3, respectively), types of hydrocolloids (sodium alginate and methylcellulose) and application methods (mixing vs. coating), on solid foam structure and oil absorption of fried rice cracker. De-proteinization of rice flours by bromelain altered the MWs of proteins towards the lower ones and reduced the protein content from 7% to 3% ($p < 0.05$). These alterations increased peak viscosity but decreased final viscosity of rice flour slurries ($p < 0.05$). In rice cracker, air cells with larger size were obtained in crackers with low protein content and those with high ratio of waxy rice flour. However, these large air cells in low protein cracker did not affect oil absorption ($p \geq 0.05$). In contrast, rice cracker with higher ratio of waxy rice flour containing air cell size of more than 1200 μm in diameter increased oil absorption ($p < 0.05$) compared with rice flour cracker. Coating rice sheet with 1% (w/v) methylcellulose before frying could effectively reduce the air cell diameter in the range of 1-900 μm and oil absorption ($p < 0.05$) compared with the non-coated ones. The understandings on the roles of size distribution of air cells on oil absorption may help formulating the low-fat fried products.

Student's signature

Thesis Advisor's signature

ACKNOWLEDGEMENTS

This thesis would not have been succeeded without valuable assistances and supports of the following people; first of all, I would like to say thank you to Assoc. Prof. Dr. Parichat Hongsprabhas, the advisor of this study. Without her valuable suggestion and encouragement, the research would have been lost somewhere around. Thank you Assist. Prof. Dr. Masubon Thongngam for valuable contribution to this thesis and Assist. Prof. Dr. Namfone Lumdubwong for method of amylose determination.

Secondly, I would like to send my gratitude to Kasetsart University under Special Research Unit: Rice and Starches and the Center of Excellence of Agricultural Biotechnology, Ministry of Education for partial supports this research financially. In material support, I would like to say thank you to TIC gums, Inc., Belcamp, USA for donating commercial methylcellulose, the crucial element in this study.

I also would like to thank Miss Nantarat Na Nakornpanom and all labmates in 2413 laboratory for their suggestions and supports. Thank you Miss Kamolwan Israkarn for micrographs from CLSM. Thank you P'Pong, P'Pard, P'Kae, P'Somporn and P'Moo for valuable support in laboratory equipments. Thank you my friends from Bodin 3, KMITNB and internship at Malee Sampran factory for their continuing encouragements.

Last but far from least, I would like to say thank you to my family for giving such great love and care. Thank you my elder sister and brother for their academic and personal supports. I could not have been in this point without you all.

Sasikarn Kithikorn

January 2009

TABLE OF CONTENTS

	Page
TABLE OF CONTENTS	i
LIST OF TABLES	ii
LIST OF FIGURES	iv
INTRODUCTION	1
OBJECTIVES	2
LITERATURE REVIEW	3
MATERIALS AND METHODS	27
Materials	27
Methods	33
RESULTS AND DISCUSSION	37
CONCLUSION AND RECOMMENDATIONS	55
LITERATURE CITED	56
APPENDICES	61
Appendix A Analytical methods	62
Appendix B Statistical analysis	74
CIRRICULUM VITAE	82

LIST OF TABLES

Table	Page
1	37
2	39
3	39
4	43
5	45
6	50
7	54
Appendix Table	
B1	75
B2	76
B3	76
B4	77
B5	78

LIST OF TABLES (Continued)

Appendix Table	Page
B6 Statistical analysis of effect of rice flour to waxy rice flour ratios and hydrocolloid addition on water content, oil absorption and expansion in rice crackers (factorial analysis)	79
B7 Statistical analysis of effect of rice flour to waxy rice flour ratios and hydrocolloid addition on water content, oil absorption and expansion in rice crackers (ANOVA)	80
B8 Statistical analysis of effect of 1 % (w/v) hydrocolloid coating on water content, oil absorption and expansion in rice crackers (RF:WF ratio = 0.7:0.3)	81

LIST OF FIGURES

Figure		Page
1	Model of solid foam structure	7
2	Formation of solid foam structure during frying process	7
3	Formation of solid foam structure in starch-based products	8
4	Structure of alginate monomers	9
5	Structure of alginate segments	10
6	Coordination of a calcium ion with two carboxyl and hydroxyl groups on adjacent G-block chains	11
7	“Egg box” model for alginate gelation promoted by calcium ions	12
8	Structure of methylcellulose	13
9	Structure of starch polymers consist of amylose and amylopectin	17
10	Diagram of various protein bodies and a compound starch granule in endosperm subaleurone layer	23
11	Complex of a segment of an amylose molecule and a molecule of fatty acid	25
12	Effect of protein content of rice flour and waxy rice flour on size distribution of air cells in rice crackers	41
13	Effect of protein content of rice flour and waxy rice flour on microstructure in rice crackers	41
14	SDS-PAGE profiles of storage rice proteins in the absence and presence of β -mercaptoethanol	44
15	Effect of rice flour to waxy rice flour ratios on the size distribution of air cells in rice crackers	46
16	Effect of rice flour to waxy rice flour ratios on microstructure in rice crackers	46
17	CLSM micrographs of rice sheets adding with 0.1 % (w/v) hydrocolloids	48

LIST OF FIGURES (Continued)

Figure		Page
18	Effect of 0.1 % (w/v) hydrocolloids addition during rice sheet preparation on size distribution of air cells and microstructure in rice crackers (RF:WF ratio = 0.7:0.3)	51
19	Effect of 1 % (w/v) hydrocolloids coating on rice sheet before frying on size distribution of air cells and microstructure in rice crackers (RF:WF ratio = 0.7:0.3)	53
Appendix Figure		
A1	Standard curve of potato amylose for amylose determination	71

FORMATION OF SOLID FOAM STRUCTURE AND OIL ABSORPTION OF FRIED SNACKS FROM RICE FLOUR COMPOSITES

INTRODUCTION

Solid foam structure is composed of small cells of air or gas dispersed in solid continuous phase. Many food products have solid foam structure, such as snack and breakfast cereal that can be produced in several ways (Aguilera, 1992; Campbell and Mougeot, 1999). The most popular and economical way to prepare solid foam in food is frying process. In frying process, sudden evaporization of water and internal steam is formed rapidly, causing the product to puff (Aguilera, 1992; Campbell and Mougeot, 1999), which leads to a low-density, porous and thin-walled structure (Aguilera, 1992). Changes in starch-based products into solid foam structure were proposed by Aguilera (1992). In raw starch system, starch granules and proteins are dispersed in aqueous phase. Then, cooking makes starches gelatinize and proteins denature, causing starch particulates to disperse in a starch-protein gel matrix. Finally, frying process makes air bubbles dispersed in starch-protein continuous matrix called “*solid foam*”.

Many factors affect size distribution of air bubbles; for example time of frying (Rajkumar *et al.*, 2003), temperature of frying (Krokida *et al.*, 2000), particle size of flour (Moriera *et al.*, 1997), degree of starch gelatinization (Kawas and Moreira, 2001) and thickness of sample (Krokida *et al.*, 2000). The rationale of this study based on the fact that solid foam structure is generated from air bubble dispersed in starch-protein matrix; therefore, controlling the viscoelastic properties of starch-protein matrix of rice sheet before frying could lead to various size of air cell, which would affect oil absorption. The viscoelastic properties of starch-protein matrix can be manipulated by controlling the degree of starch gelatinization and interactions with proteins.

OBJECTIVES

1. To control viscoelastic properties of starch-protein matrix of rice sheets by altering flour composition using different protein contents and ratios of rice flour to waxy rice flour, which subsequently controlled amylose to amylopectin ratio.

2. To regulate the air cell size distribution and oil absorption by using hydrocolloids, mixing of hydrocolloids during rice sheet preparation and coating the hydrocolloids onto rice sheet before frying.

LITERATURE REVIEW

1. Factors affecting solid foam structure and oil absorption in frying products

Deep-fat frying process produces fried products with crispy texture, golden brown color and desired flavor, which further improved overall food palatability and satisfied consumers (Mellema, 2003; Moyano and Pedreschi, 2006). Their characteristics make consumers to eat them more than their needs. Furthermore, fried products contain high amount of fat, up to 1/3 of total food product by weight, which associated with many chronic diseases such as obesity and coronary heart diseases (Mellema, 2003). To make fried products more acceptable for health-conscious consumers, fat should be reduced (Khalil, 1999).

Apart from fat absorption of fried products, the increase surface area in solid foam structure should be emphasized. The quality of fried products depends on their structural, textural and optical properties. Most important structural properties, such as apparent density, true density and porosity of fried products, changed during frying. Changes in oil and water content with frying time was related to structure (pore size and distribution) of samples, of which porosity increases during frying process (Krokida *et al.* 2000). The porosity of the product formed during frying plays an important role in the subsequent oil uptake (Yamsaengsung and Moriera, 2002). Because of the heterogeneity and complex structure of the porous material, the oil appears to be distributed randomly throughout the fried product such as tortilla chips after frying, especially at the puffed areas of the chips (Moriera *et al.*, 1995). Therefore, a better understanding of the solid foam structure and their oil absorption could provide ways to optimize the porosity of fried product, thus the control of oil absorption.

Solid foam structure and oil absorption, which related to overall surface area of fried food, are affected by time and temperature of frying, particle size of flour, degree of starch gelatinization and thickness of sample as follows:

1.1 Frying time

Rajkumar *et al.* (2003) reported that the pore sizes of steam-baked tortilla chips were developed according to frying time. Tortilla chips, a triangle shape snack, were produced from corn flour, vegetable oil, salt and water (Anonymous, 2006). Steam-baked tortilla chips, which were subjected to starch gelatinization prior to frying, were fried for 0, 10, 20, 40 and 60 s. It was found that increasing times of frying resulted in a higher mean pore volume to 43.77, 81.36, 156.61, 252.48 and 282.64 μm^3 , respectively. This result showed that longer time of frying led to an increase in mean pore size due to the loss of water from three-dimensional matrix, which was partly replaced by oil and air, resulting in an increase of air cell sizes and puffing of final fried products.

1.2 Frying temperature

Krokida *et al.* (2000) showed that the oil temperature affected structural properties such as apparent density, true density and internal porosity of potato french fries. Further, mathematical model was used to correlate those properties with oil and moisture contents. Potatoes were cut into strips with 10×10×40 mm in dimension and blanched at 70°C for 10 min. The potato strips were fried in a mixture of 1:1 refined to hydrogenated cotton seed oil for 0.3, 0.6, 1, 3, 5, 7, 10, 13, 15 and 20 min. Frying temperature was set at 150°C, 170°C and 190°C. The results showed that increasing oil temperature led to a decrease in true density due to higher oil content and lower water content of potato strips. More intense mass transfer phenomena from higher oil temperature caused an increase in water vaporization, air pore development and oil uptake. These characters led to a lower apparent density and higher porosity of french fries as temperature increased.

1.3 Particle size of flour

Moriera *et al.* (1997) reported that tortilla chips made from flours with various sizes of fine (passed through U.S. #100 sieve), intermediate (passed through U.S. #70 sieve but not #100), coarse (not passed through U.S. #70 sieve) and control (33.3% fine, 21.4% intermediate and 45.3% coarse) particle size of flours had different oil absorption and appearance. Normally, tortilla chips were produced by mixing corn flour with water, sheeting and forming of triangular pieces, baking to raw tortilla chips and deep-fat frying to tortilla chips. In this experiment, all treatments of tortilla chips were fried with soybean oil at 190°C for 60 s and they had the same initial moisture content of around 60 % dry basis. Moriera *et al.* (1997) found that tortilla chips made from fine, intermediate, coarse and control particle size of flours had final oil content (dry basis) of 45.97%, 31.30%, 27.73% and 33.97%, respectively. Moreover, tortilla chips prepared from flour with fine particle size showed excessive puffing and pillowing, resulting in higher oil absorption. The lowest oil content and no puffing presented in tortilla chips prepared from flour with coarse particle size. These results showed that flour with coarse particle size caused low oil absorption of tortilla chips with no puffing.

1.4 Degree of starch gelatinization

Kawas and Moreira (2001) observed that the degree of starch gelatinization related with final oil content of the tortilla chips and the product quality attributes. Tortilla chips was prepared using starch with different degree of starch gelatinization before frying; i.e. 5%, 45% and 87% degree of gelatinization determined by Differential Scanning Calorimetry (DSC). All pre-frying conditions resulted in the same initial moisture content of tortilla chips of approximately 42% wet basis. They found that the degree of starch gelatinization affected product quality attributes, which were porosity, puffiness and pore-size distribution of tortilla chips. After frying, the sample with low degree of gelatinization (5%) gave rise to the tortilla chip with 0.33 of porosity. Tortilla chips prepared from raw materials with 45% of starch gelatinization and with 87% of starch gelatinization had porosity of 0.55 and

0.70, respectively. The low degree of starch gelatinization facilitated vapor to escape from the chips during frying and then allowed more oil to enter free spaces, causing little puffiness or no pillowing because there was no area of excess pressure build up. This consequently resulted in high final oil content. The high degree of gelatinization before frying formed a tight barrier of the outer surface of the steamed-baked chips. During puffing, tight barrier created pockets as water vapor tried to escape from the interior of chips and blocked the oil absorption, leading to tortilla chip with low oil content. These results showed that tight barrier led to large pocket or high puffiness, consequently low oil uptake in finished fried product.

1.5 Thickness of sample

Krokida *et al.* (2000) reported that structural properties such as apparent density, true density and internal porosity in french fries potatoes were affected by sample thickness. These properties were correlated with oil and moisture content. Increasing sample thickness of potato strips resulted in lower oil content and higher water content for the same frying time; thus true density increased. Apparent density increased and porosity decreased with thicker sample. This was due to the lowering of water vaporization, air pore development and oil uptake from reducing mass transfer phenomena.

2. Mechanisms of solid foam structure formation from frying process

As mentioned above, oil absorption and solid foam structure were the crucial quality attributes of fried products. Therefore, mechanisms of solid foam structure formation during frying process have been studied by several authors. Basically, solid foam structure is composed of small cells of air or gas dispersed in solid continuous phase (Figure 1). Many food products have solid foam structure, such as snack and breakfast cereal that can be produced in several ways (Aguilera, 1992; Campbell and Mougeot, 1999).

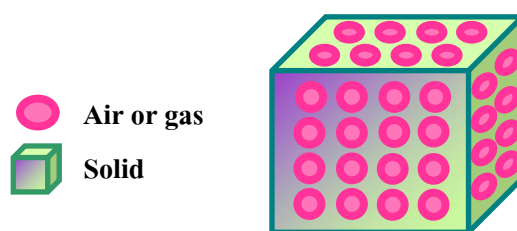


Figure 1 Model of solid foam structure.

Source: Aguilera (1992)

The most popular and economical way to prepare solid foam in food is frying process. In frying process, a sudden evaporation of water and internal steam is formed rapidly, causing the product to puff (Aguilera, 1992; Campbell and Mougeot, 1999). This leads to a low-density, porous and thin-walled structure (Aguilera, 1992) as showed in Figure 2.

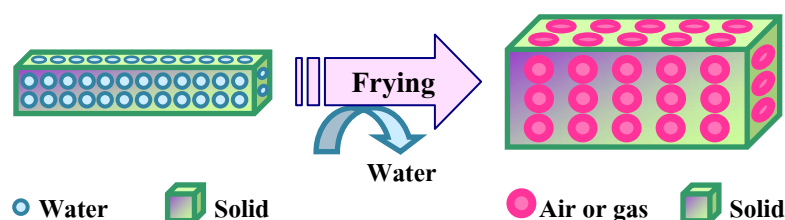


Figure 2 Formation of solid foam structure during frying process.

Changes of starch-based products into solid foam structure were proposed by Aguilera (1992) (Figure 3). In raw starch, starch granules and proteins are dispersed in aqueous phase. Then, cooking with sufficient heat and water results in starch gelatinization and protein denaturation, causing starch particulates to disperse in a starch-protein gel matrix. Finally, frying process makes air bubble dispersed in starch-protein continuous matrix called “*solid foam*”, solidifying starch-protein gel matrix and trapping air bubble created from water. The water in the products evaporated into steam, which expanded the three-dimensional matrix during frying process.

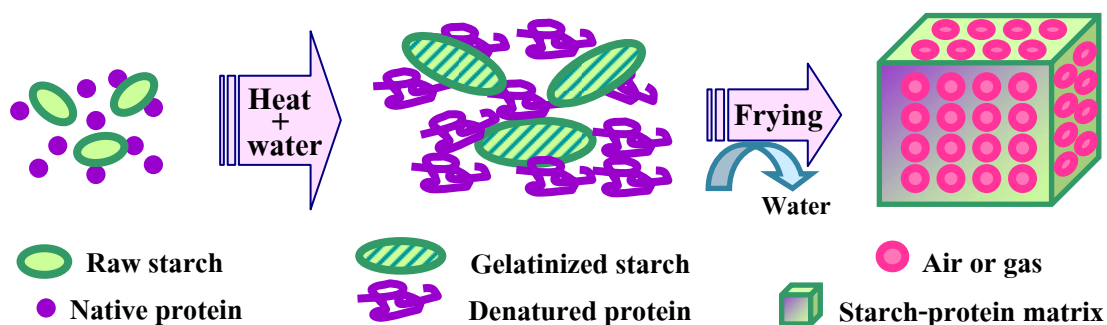


Figure 3 Formation of solid foam structure in starch-based products.

Source: Aguilera (1992)

These changes implicate that incorporation of starch and protein in matrix with different viscoelastic properties may control the formation of solid foam structure which different porosity and oil uptake during frying. Evaporation of water resulted in oil absorption that replaced water vapor and the porosity of final-fried product was generated (Mellema, 2003). Therefore, manipulating starch-protein matrix before frying may help regulating oil absorption in finished fried products.

3. Use of hydrocolloids in fried products

The integrity of starch granules can be controlled by water content in the system. Therefore, addition of hydrocolloid, which has high water hydration, results in a slow down in the loss of starch granule integrity (Hongsprabhas *et al.*, 2007), and may further reduce oil absorption if the concentration of hydrocolloid was high enough.

Hydrocolloids used in this study included alginate and methylcellulose with different characteristics and molecular structures as follows:

3.1 Alginate

Alginate occurs as the major structural polysaccharides in the cell walls and intercellular spaces of brown algae known as *Phaeophyceae* (Onsøyen, 1992; Nisperos-Carriedo, 1994). Alginic acid, the free acid form of alginate, is the intermediate product in the commercial manufacture of alginates. Alginic acid has limited stability. In order to make stable water-soluble alginate products, the alginic acid is transformed into commercial alginates by incorporating different salts, such as sodium carbonate (Na_2CO_3) to form sodium alginate (Onsøyen, 1992).

Alginates, the high molecular weight linear polymers, are salts of alginic acid with different degrees of polymerization within the range of 100-3,000 monomers corresponding to molecular weights of approximately 20,000-600,000 Da. The building blocks of alginic acid are the sugar acid of β -D-mannuronic acid (M) existed in the ${}^4\text{C}_1$ conformation (Figure 4a) and α -L-guluronic acid (G) existed in the ${}^1\text{C}_4$ conformation (Figure 4b). These sugars are connected in alginate polymer to their neighboring units through (1,4) glycosidic bonds (Sime, 1990; Onsøyen, 1992; Whistler and BeMiller, 1999).

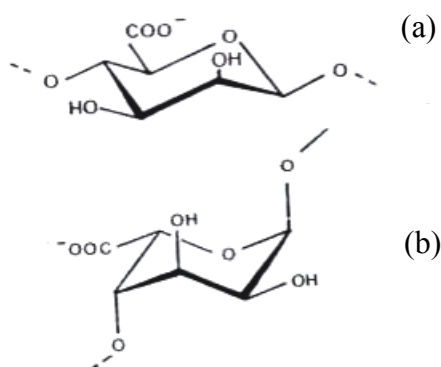


Figure 4 Structure of alginate monomers are composed of (a) β -D-mannuronic acid (M) in ${}^4\text{C}_1$ conformation and (b) α -L-guluronic acid (G) in ${}^1\text{C}_4$ conformation.

Source: Onsøyen (1992)

The two monomeric units could occur in homogeneous regions, which consisted of only one of the two units as MMMM and GGGG, and in heterogeneous regions containing both units as MGMG. Segments containing only monomeric M-residues linked together with β -(1,4) glycosidic bond are referred to as M-blocks (Figure 5a) and those containing only monomeric G-residues linked together with α -(1,4) glycosidic bond as G-blocks (Figure 5b). MG-blocks contain the two units in a mixed arrangement (Figure 5c). These different blocks give quite different chain conformations. The carboxylic groups are responsible for an equatorial/equatorial glycosidic bond in M-M resulted in flexible ribbon-like polymer in the M-block regions; an axial/axial glycosidic bond in G-G resulted in buckled and stiff polymer in the G-block regions. An equatorial/axial glycosidic bond in M-G resulted in intermediate stiffness in the M-G block regions. Different percentages of the different block segments cause alginates from different seaweeds to have different properties (Onsøyen, 1992; Whistler and BeMiller, 1999). High-G alginates form strong, brittle gels with a tendency to syneresis, whereas high-M alginates form weaker and more elastic gels, and less prone to syneresis (Sime, 1990).

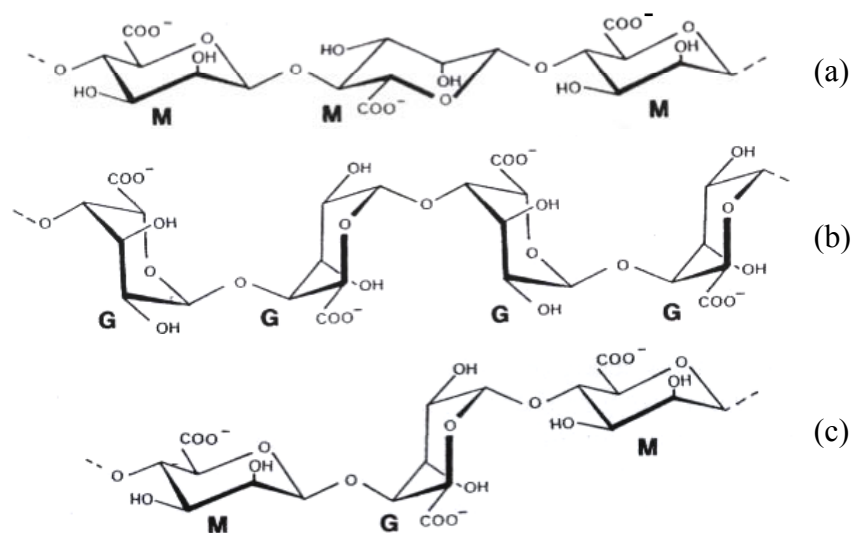


Figure 5 Structure of alginate segments; (a) M-blocks, (b) G-blocks and (c) M-G blocks.

Source: Onsøyen (1992)

Alginate has negative charges due to the presence of carboxylic groups with linear structure. It has optimum pH for solubilization in the range of 2.8-10 ($pK_a = 3.4-4.4$) and optimum soluble solids in the range of 0-80 %. Alginate gelation occurs in the presence of calcium ion (Ca^{2+}) around 20-70 mg per gram of alginate or at pH below 4 (Trudso, 1991).

Gelation of sodium alginate solution occurs upon the addition of calcium ions. Sodium in sodium alginate is exchanged with calcium, resulting in calcium ions filled cavities that formed between parallel G-block chain regions (Onsøyen, 1992; Whistler and BeMiller, 1999). These cavities contain two carboxylate and two hydroxyl groups, one of each from each chain. The calcium ion interacts not only with carboxyl groups but also with the electronegative oxygen atoms of the hydroxyl groups (Figure 6). The result is a junction zone that has been called an “egg box” upon the arrangement (Figure 7), with the calcium ions being linked as eggs in the pockets of an egg carton. Strength of the gel depends on the content of G-blocks in alginate used and the concentration of calcium ions. Alginate gels are heat-stable and thermo-irreversible. Once set it will not melt upon reheating (Sime, 1990; Whistler and BeMiller, 1999). Moreover, alginate has the ability to gel at low temperature. As decreased temperature, gelation occurs because calcium induced interchain associations (Sime, 1990; Onsøyen, 1992).

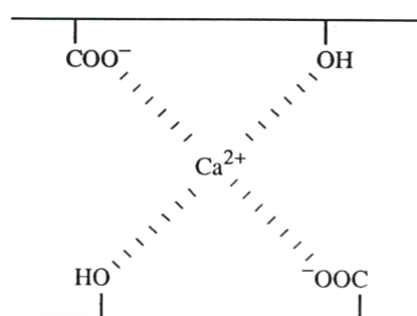


Figure 6 Coordination of a calcium ion with two carboxyl and hydroxyl groups on adjacent G-block chains.

Source: Whistler and BeMiller (1999)

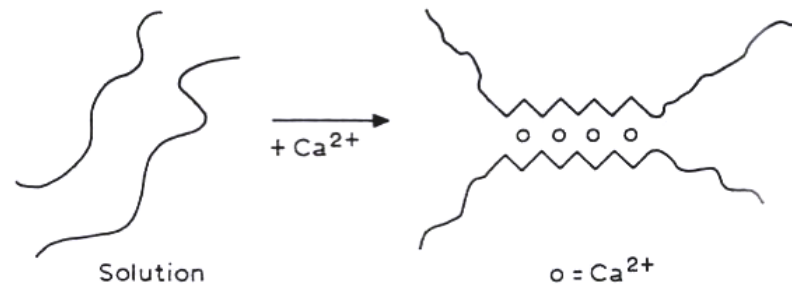


Figure 7 “Egg box” model for alginate gelation promoted by calcium ions.

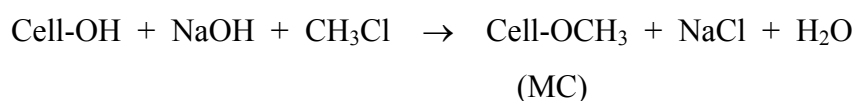
Source: Sime (1990)

Since alginate molecules are the salts of weak carboxylic acids, with pK_a values of 3.38 for mannuronic acid, 3.65 for guluronic acid and 3.5 for alginic acid. Decreasing of pH value causes reduction of carboxyl group ionization, especially at the pH values of 3 or less. This loss of ionization at low pH values causes taking up protons of alginate chains and losing of their negative charges, which gives more neutral molecules and consequently allows junction zones to develop. As molecular associations increase, the viscosity of the solution increases. Finally, when the pH is low enough, alginic acid precipitates from solution because of the extensive intermolecular associations (Onsøyen, 1992; Whistler and BeMiller, 1999).

The safety of alginic acid and its sodium salts is not specified for Acceptable Daily Intake (ADI). Sodium alginate used as stabilizer is generally recognized as safe (GRAS). Moreover, alginates can be used in all foodstuffs under *the Quantum Satis*, which means “no maximum level of the additive in or on a food is specified but in or on a food the additive may be used in accordance with good manufacturing practice at a level not higher than is necessary to achieve the intended purpose and provides that such use does not mislead the consumers” (Draget, 2000).

3.2 Methylcellulose

Methylcellulose (MC) is a cellulose derivative. To prepare MC, alkali cellulose is formed by mixing cellulose (Cell-OH) with aqueous caustic NaOH, and then the alkali cellulose is reacted with methyl chloride (CH₃Cl), and MC (Cell-O-CH₃) is created by replacing protons of some hydroxyl groups with methyl groups (Zecher and van Coillie, 1992; Whistler and BeMiller, 1999). This reaction is described in equation below:



MC is white to off-white creamy solids with neutral taste and odor. It is cold-water soluble because the protrusions of the methyl ether group along the chains prevent the intermolecular association characteristic of cellulose. A minimum degree of substitution (DS), required for water solubility of MC, is about 1.4. Commercial MC has average DS ranging from 1.4 to 2.0 (Figure 8) (Zecher and van Coillie, 1992; Whistler and BeMiller, 1999).

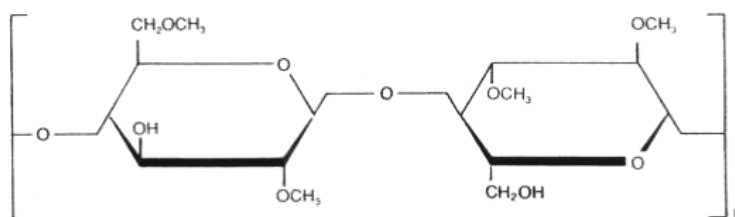


Figure 8 Structure of methylcellulose (DS = 2).

Source: Zecher and van Coillie (1992)

While a few ether groups spreading along cellulose molecules enhance water solubility by preventing chain association, they also decrease chain hydration by replacing water-binding hydroxyl groups with less polar ether groups. Thus, the ether groups restrict the hydration of the chains to the point that they are on the

borderline of water solubility. Solution viscosities decrease as temperature increases until the thermal gel point is reached. Hence, when an aqueous MC solution is heated, the water molecules solvating the polymer molecules are given sufficient kinetic energy and separate from the chain, allowing intermolecular associations with hydrophobic interaction of methyl groups. This results in gelation of MC at the temperature ranging from 50 to 90°C. Reducing the temperature once again brings about rehydration and solubility. Thus, this thermal gelation of MC is thermo-reversible. MC solution is stable over a wide pH range of 2-11, in which viscosity is nearly independent on pH. This property is the basis for many applications of MCs. Therefore, MC is a nonionic, water-soluble ether yielding tough and flexible transparent films owing to the linear structure of the polymer backbone (Zecher and van Coillie, 1992; Nisperos-Carriedo, 1994; Whistler and BeMiller, 1999; Williams and Phillips, 2000).

Although, the MC film has high transparency and tensile strength with water soluble character, it is insoluble in most organic liquids such as fats and oils. MCs can also be used to reduce the amount of fat in food products through two mechanisms. They impart fatlike properties with least hydrophilic of the cellulose ethers so that the fat content of a product can be reduced. Furthermore, they reduce absorption of fat while frying due to the fact that gel structure produced by thermogelation providing a barrier to oil. Therefore, oil resistance and thermogelation properties are used to reduce oil pick-up during deep-fat frying (Zecher and van Coillie, 1992; Nisperos-Carriedo, 1994; Whistler and BeMiller, 1999). MC has been permitted the use levels in term of *the Quantum Satis*. Modified cellulose is not specified for ADI (Murray, 2000).

3.3 Influences of hydrocolloids on oil uptake

Many studies have proposed hydrocolloid application to reduce oil absorption in various kinds of fried products. Mallikarjunan *et al.* (1997) had observed that coatings with different types of edible films can reduce oil pick-up in mashed potato balls. Corn zein (CZ), hydroxypropylmethylcellulose (HPMC), and MC, were used as edible films. Among all films tested, the effectiveness in reduction of oil absorption was found in samples coated with MC. The oil absorption could be reduced to 59.0 %, 61.4 % and 83.6 % of the uncoated samples when coated with CZ, HPMC and MC, respectively.

Khalil (1999) found that two-step coating was more effective to reduce oil uptake than one-step coating. French fries were coated with calcium chloride and either pectin or sodium alginate at different concentrations for first coating. Then, the single coated treatment, which resulted in the lowest oil content, was selected to continue for the second coating with carboxymethylcellulose (CMC). Compared with the uncoated one, the first coating with 0.5% calcium chloride and 5 % pectin and the additional second coating with 1.5 % CMC in french fries could reduce 54 % of oil absorption, while single coating with the same hydrocolloids reduced only 40 % of oil content.

Garcia *et al.* (2002) reported that deep-fat frying potato strips coated with MC and HPMC reduced oil absorption. Coating of MC was more effective in reducing oil absorption than HPMC. MC, which is potential hydrocolloid in lowering oil uptake, was added with sorbitol as a plasticizer in potato strips and dough discs. Coating potato strips with 1 % MC and 0.51 % sorbitol and coating the dough discs with 1 % MC and 0.75 % sorbitol reduced 40.60 % and 35.20 % of oil absorption, respectively, compared with the uncoated samples.

It was apparent that the types and concentrations of hydrocolloids affected oil absorption differently.

4. Characteristics of rice flour and waxy rice flour

Rice (*Oryza saliva* L.) is a member of the family *Poaceae* (formerly *Gramineae* or grass), harvested as paddy rice. Removal of the bran layers (pericarp, tegmen, nucellus, and aleurone) along with polish (subaleurone), germ (embryo), and a small part of the endosperm results in milled rice or white rice composed entirely of endosperm, with a starch content approximately 78 % wet basis (14 % moisture content) or 90 % dry basis. Other constituents in wet basis (14 % moisture content) are 4.5-10.5 % of crude protein (N \times 5.95), 0.3-0.5 % of crude fat, 0.2-0.5 % of crude fiber and 0.3-0.8 % of crude ash (Champagne *et al.*, 2004). Milled rice or white rice was normally produced into flour. Different types of rice flour contained different compositions. The different constituents of flour also affected starch granule integrity and could subsequently result in solid foam structure and oil absorption of fried products.

4.1 Starch

Carbohydrate in rice is stored in the form of starch, which is one of the nature's energy reserves. Starch occurs naturally as discrete particles called granules. The size and shape of starch granule depends on botanical source. Rice starch granules have average size about 2-9 μ m in the form of polygonal. Starch is composed of two polymers; linear polysaccharide called amylose and highly branched polysaccharide called amylopectin (Figure 9) (Appelqvist and Debet, 1997; Whistler and BeMiller, 1999; Champagne *et al.*, 2004).

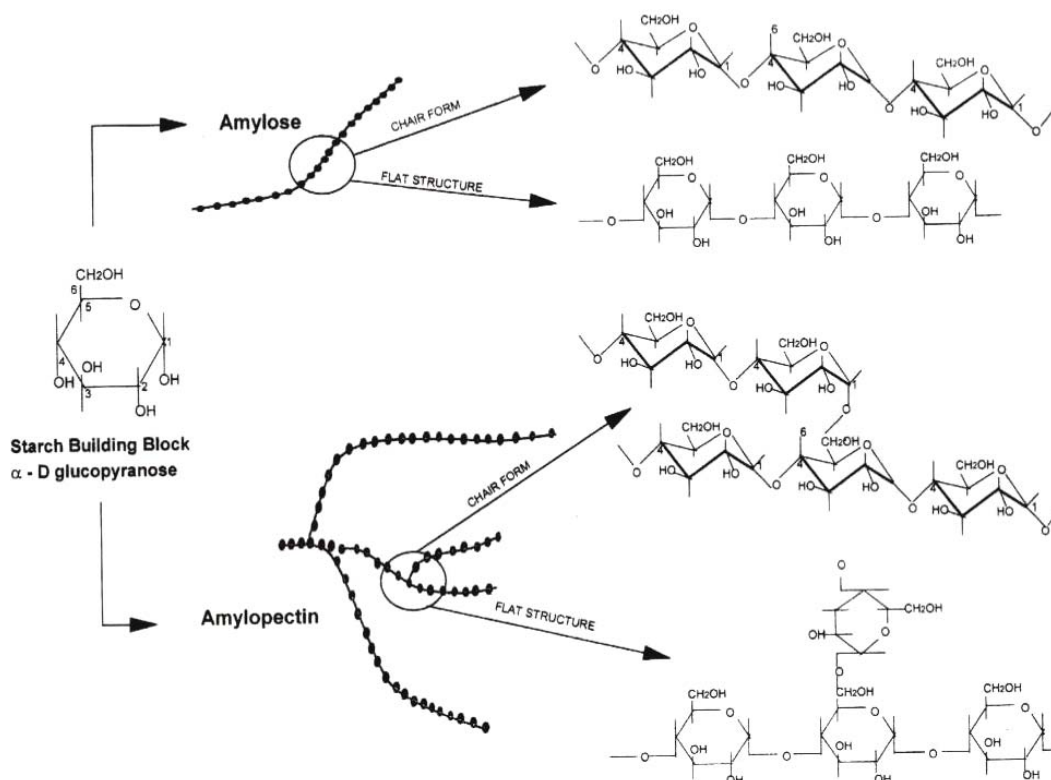


Figure 9 Structure of starch polymers consist of amylose and amylopectin.

Source: Murphy (2000)

Amylose is a linear chain of (1→4)-linked α -D-glucopyranosyl units and many amylose molecules have a few α -D-(1→6) branches for about 0.3-0.5% of total linkages. The branches in branched amylose molecules are either very long or very short and the branch points are separated by large distances, allowing the molecules to act as linear polymer, forming strong films and easily retrogrades. The degree of polymerization (DP) ranges from 10^2 to 10^4 , giving molecular weights from 10^4 to 10^6 Da, usually more than 10^5 Da (Rapaille and van Hemelrijck, 1992; Whistler and BeMiller, 1999). Nonwaxy rice starch has amylose content of 8-37%, whereas the amylose content of waxy rice starch ranges from 0.8-1.3% (Fitzgerald, 2004). The axial/equatorial position coupling of the (1→4)-linked α -D-glucopyranosyl units in the amylose chains gives the molecules a right-handed spiral or helical shape. The interior of the helix is lipophilic contained predominantly hydrogen atoms, while the

hydroxyl groups are positioned on the exterior of the coil (Whistler and BeMiller, 1999).

Amylopectin is a very large and highly branched molecule. It is composed of a chain of α -D-glucopyranosyl units joined by (1 \rightarrow 4) linkages and α -D-(1 \rightarrow 6)-linked branch with a linear chain of 40-50 units. The branch point linkages constitute 4-5 % of the total linkages. DP of amylopectin is greater than 50,000, yielding molecular weights of approximately 10^7 Da or more (Rapaille and van Hemelrijck, 1992; Whistler and BeMiller, 1999). An amylopectin molecule consists of a main chain, called the C chain. It carries one reducing end-group and numerous branches, termed B chains, to which one to several third-layer A chains are attached. B-chains are connected to another chain via (1 \rightarrow 6) linkages and also have one or more A or other B chains attached to them via (1 \rightarrow 6) linkages. A chains are connected to another chain via (1 \rightarrow 6) linkages, but they unbranched (Whistler and BeMiller, 1999). The branches of amylopectin molecules are clustered and occur as double helices due to pairs of non-reducing chain ends in clusters, entwined around each other in parallel double helices. At least, some branches of linear segments of amylopectin molecules have the same right-handed α -helix conformation found in amylose molecules. Amylopectin constitutes about 75 % of most common starches and is considered as a skeleton of the starch granule. Some starches consist entirely of amylopectin, called waxy or glutinous starches (Whistler and BeMiller, 1999; Fitzgerald, 2004).

Starch granules are made up of amylose and/or amylopectin molecules. They combine with one another to form a compact and ordered mass. The region of ordered molecules continues to grow in a radial direction from the growth center, called hilum. Completed granules with molecules arranged in a radial direction contain both crystalline and noncrystalline regions in alternating layers, described as semicrystalline. This granular structure occurs by the clustered branches of amylopectin form packed double helices. Packing together of these double helical structures form many small crystalline regions in a dense layer of starch granules

alternated with amorphous regions. This noncrystalline region is rich in amylopectin branch points and is also likely to contain amylose (Whistler and BeMiller, 1999; Fitzgerald, 2004). Moreover, amorphous areas occur in starch granules are channels extending from the outer surface to the center of the granule called surface pores, which have been observed in starch granules from rice. Channels are thought to extend from the surface pores, facilitating the exchange of water to and from the starch granule and providing exit points for amylose to leach during gelatinization of starch (Fitzgerald, 2004). Amylopectin molecules forming the principle structure of the granule are arranged with their reducing ends toward the center of the granule, while the starch granule surface contains the nonreducing end-groups from amylose and amylopectin (Eliasson and Gudmundsson, 1996; Whistler and BeMiller, 1999). The radial and ordered arrangement of starch molecules in a granule is evident from the white maltese cross on a black background of granules under cross polarized light, called birefringence. The center of the cross is at the hilum, the origin of growth of granule (Whistler and BeMiller, 1999).

Starch granules are dense and insoluble, but it can imbibe cold water reversibly. They can slightly swell on hydrating cold water and then return to their original size upon drying. As they are heated in the presence of water beyond the reversible point, molecular order within starch granules is disrupted, which referred to gelatinization. This phenomenon occurs when heating a starch-water suspension. Molecules within granules vibrate and twist so violently causing intermolecular hydrogen bond break and replaced hydrogen bonds with water molecules, producing more extensive hydration layers around the separating molecules. Thus, starch chains become sheathed in layers of water molecules that allow them to move more freely. Eventually, molecular segments move to distances and positions that make it impossible for them to return to their original positions upon dehydration and subsequently swelling of granules to several times their original size. Evidence for the loss of organized structure includes loss of birefringence and irreversible granule swelling due to the breakage of hydrogen bonds between starch molecules (Nisperos-Carriedo, 1994; Eliasson and Gudmundsson, 1996; Whistler and BeMiller, 1999). The disappearance of 90-95 % of these crystallinities upon heating a starch

suspension is used to determine the endpoint of gelatinization temperature. Rice has been reported to have gelatinization temperature from 55 to 79°C (Bergman *et al.*, 2004). Continued heating of starch granules in excess water results in further granule swelling, additional leaching of soluble components (primarily amylose), and eventually, total disruption of granules, especially with the application of shear forces. This phenomenon results in the formation of a starch paste, which is a viscous mass, consisting of a continuous phase of solubilized amylose and/or amylopectin and a discontinuous phase of granule remnants, granule ghosts and fragments. The ghost is the remnant remaining outer portion of the granule, while the inner portion is solubilized after cooking. It appears as an insoluble outer envelope, but is not a membrane (Whistler and BeMiller, 1999).

Cooling a hot starch paste generally produces gel, rice starch produce opaque gel while waxy rice starch are clear and cohesive gel (Whistler and BeMiller, 1999), resulted from junction zone formation. The formation of junction zones can be considered to be the first stage of an attempt by starch molecules to recrystallize. The changes that occur in gelatinized starch, from initially an amorphous to a more ordered or crystalline state, are termed retrogradation. These changes occur because gelatinized starch is not in thermodynamic equilibrium. The rheological properties will change, as evident by increased firmness or rigidity (Eliasson and Gudmundsson, 1996; Whistler and BeMiller, 1999). Loss of water-holding capacity and restoration of crystallinity will also become evident and increase on aging. Retrogradation of cooked starch involves both of the two constituent polymers, amylose and amylopectin, with amylose undergoes retrogradation at a much more rapid rate than does amylopectin. Amylose retrogradation may be largely completed by the time the product cooled to room temperature. Crystallization of amylose reaches equilibrium after 2 days. Retrogradation of amylopectin is believed to involve primarily association of its outer branches and requires a much longer time than amylose retrogradation. Therefore, retrogradation of amylopectin increases slowly with time after the product is cooled. Crystallization of amylopectin approaches equilibrium after 30-40 days. Upon heating at 90°C, fully retrograded starch gel loses their crystallinity for about 70%; whereas retrogradation of amylose gel reduces for only

25% causing amylose crystals melt only above 100°C. Crystallinity of amylopectin gel is fully reversible upon heating, if the retrograded gel is exposed to a temperature greater than the gelatinization temperature of crystalline amylopectin (Eliasson and Gudmundsson, 1996; Whistler and BeMiller, 1999; Fitzgerald, 2004).

Rapid Visco Analyser (RVA) has become the standard method determining rice pasting properties (Bergman *et al.*, 2004). In the initial stages of this procedure, the temperature is below the gelatinization temperature of starch suspension and the viscosity is low. When the temperature rises above the gelatinization temperature of starch suspension, almost all water is absorbed within the starch granules causing them to swell and the viscosity increases. The temperature at the onset of this rise in viscosity is known as “pasting temperature”. Granules swell over a range of temperatures, the granules disrupt (with shear) and the more-soluble starch leaches out into solution, which are primarily amylose and some amylopectin. “Peak viscosity” is usually achieved soon after the heating cycle reaches 95°C. During the holding period of the test, the sample is subjected to constant temperature at 95°C over a certain time range with applied mechanical shear. This process further disrupts the granules, with accompanying starch leaching and subsequent polymer alignment. This period is accompanied by the reduction in viscosity; the minimum value reached is called “trough” or “holding strength”. As the mixture is subsequently cooled, reassociation between starch molecules occurs to a greater or lesser degree. This results in the formation of a paste with increasing viscosity. The viscosity at the end of the test is called “final viscosity”. This phase of the pasting curve involves retrogradation or the reordering of starch molecules (Whistler and BeMiller, 1999; Bergman *et al.*, 2004).

Apart from carbohydrate, starch also retains non-starch components, including protein and lipid. These components may affect solid foam structure and consequently oil absorption of final products.

4.2 Protein

Protein is the second most abundant constituent in milled rice (Champagne *et al.*, 2004). It has an important role in flour properties and their products. Protein is nonuniformly distributed in rice grain. There are greater concentrations in bran and periphery of the endosperm and lesser quantities towards the center of the grain (Hamaker, 1994). Protein presents in endosperm, some proteins are bound to the granule and at least in the part of residual synthase enzyme (Whistler and BeMiller, 1999).

Protein content is usually calculated from Kjeldahl nitrogen multiplied by the factor of 5.95. This factor is based on 16.8 % nitrogen content of glutelin, which is a major protein in rice (Shih, 2004). Rice proteins are classified into 4 fractions on the basis of their solubility in specific solvents; consisted of 3.8-8.8 % of the total protein in water-soluble proteins or albumins, 9.6-10.8 % of the total protein in salt-soluble proteins or globulins, 2.6-3.3 % of the total protein in alcohol-soluble proteins or prolamins and 66.1-78.0 % of the total protein in alkali-soluble proteins or glutelins (Hamaker, 1994). Therefore, rice protein is primarily composed of glutelin.

Ju *et al.* (2001) reported the isoelectric pH and denaturation temperature of long grain rice flour containing 8.75 % protein. Isoelectric points of rice proteins were measured by turbidity method at 320 nm with pH ranging from 3 to 10. They found that rice proteins had isoelectric pH about 4.1 in albumin, 4.3 in globulin and 4.8 in glutelin. However, prolamins had no isoelectric pH, but it was precipitated by adding acetone. They also measured denaturation temperatures of rice proteins. The denaturation temperatures of albumin, globulin and glutelin were 73.3, 78.9 and 82.2°C, respectively. No denaturation temperature was detected for prolamins.

Starchy endosperm contains storage protein in the form of spherical bodies (Figure 10). Three types of protein bodies are identified; large spherical, small spherical and crystalline that diameter sizes are 1-2 μm , 0.5-0.75 μm and 2-3.5 μm , respectively. Small spherical bodies are more numerous than large spherical bodies in

the starchy endosperm; while central region contains only large spherical protein bodies. The large spherical protein bodies are a deposition site for prolamin as well as glutelin proteins, while small spherical protein bodies are primarily glutelin. Rice endosperm contains large amount of protein existing as an intergranular matrix or network, connecting protein fibrils between protein bodies (Hamaker, 1994; Champagne *et al.*, 2004).

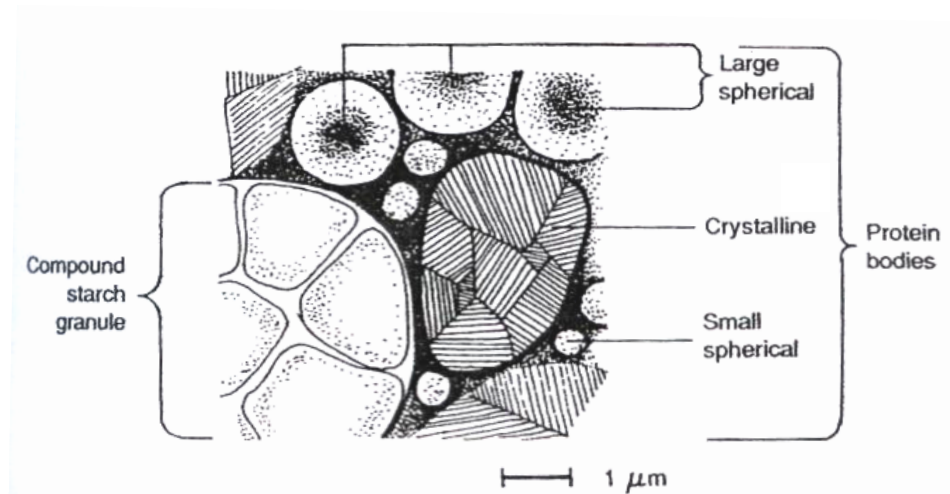


Figure 10 Diagram of various protein bodies and a compound starch granule in endosperm subaleurone layer.

Source: Shih (2004)

Proteins in the endosperm may form a barrier for the expansion of starch granules during gelatinization. The barrier for granular swelling is continuous protein matrix surrounding starch granules. Another constraint to starch gelatinization during the cooking process may be the presence of proteins closely associated with the granule. It is conceivable that starch granule-associated protein can affect the starch granule gelatinization and the granule maintains its shape even when swollen. These proteins can be found either in the form of a sparse matrix closely associated with the granule or a protein embedded inside the granule (Hamaker, 1994).

Therefore, proteins presented in endosperm might retain starch granule integrity, leading to the characteristics of starch-protein matrix, which affected the solid foam structure and oil pick-up of final fried product.

4.3 Lipid

Most of the lipids, which appear in trace constituent, in the rice endosperm are associated with protein bodies, but it is believed that starch granules also have bound lipids. Lipids are generally classified into non-starch lipids and starch lipids. Non-starch lipids represent the majority of the lipids presented in rice. Starch lipids have considerable importance relative to starch functionality, although they represent a relatively small proportion of the total lipid composition of rice (Godber and Juliano, 2004).

Lipids can form complexes with amylose by inclusion fatty acid chain within an amylose single helix (Figure 11), and perhaps by complexing with amylopectin. The helical complexes contain approximately six glucosyl units and six hydrocarbon methylene groups $[-(\text{CH}_2)_6-]$ per helical turn. Polar lipids can complex at almost any point over the entire length of amylose molecules. Up to 86 % of the glucosyl units may be complexed in amylose molecules saturated with a lipid. Amylopectin can bind only about 15 % as much lipid per unit weight. Complexation is restricted from the outer chains of amylopectin. This amylose-lipid interaction contributes to suppress melting of the crystalline regions and loss of birefringence of starch granules, to inhibit granular swelling and leaching of amylose, to retard starch gelatinization, to lower paste viscosity, to a more opaque gel and to inhibit the crystallization of starch molecules associated with the retrogradation process in cereal starches (Whistler and BeMiller, 1999).

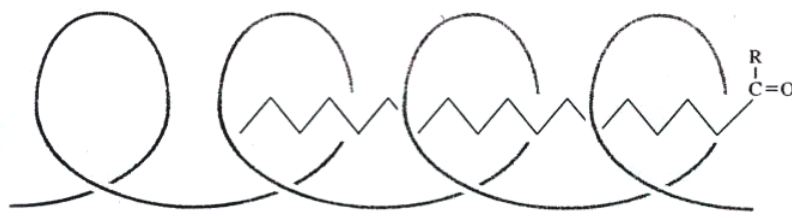


Figure 11 Complex of a segment of an amylose molecule and a molecule of fatty acid.

Source: Whistler and BeMiller (1999)

Iodine can form complexes with amylose and amylopectin molecules. Amylose chains are helical with hydrophobic or lipophilic interiors. They can form complexes with linear hydrophobic portions of molecules that can fit within the interior of the helix. The long helical segments of amylose allow long chains of polyiodine to form, producing the blue color, as found in normal or nonwaxy starch. Short-branched chains of amylopectin can also interact with iodine and give reddish-purple, as found in waxy starch. These properties of iodine-amylose and/or iodine-amylopectin complexes are a diagnostic test for starch molecules (Whistler and BeMiller, 1999; Fitzgerald, 2004).

At high or intermediate water contents, amylose-lipid complexes melt at 100-120°C. The transition is reversible due to the fact that this complex is reformed on cooling. Therefore, amylose-lipid complex might form in food processing, but it might also be present in native cereal starches (Eliasson and Gudmundsson, 1996).

Pinthus *et al.* (1998) observed that the formation of amylose-lipid complex occurred during food processing. They compared baking and frying process in core and crust region of corn starch patties to study the formation of amylose-lipid complex. These patties were prepared from 25 % (by weight) corn starch, which were heated and frozen before further process. They found that resistant starch was 5.4 % of total starch in core region of samples after 15 min of frying and 5-5.4 % of total

starch in core and crust region of samples after 20-80 min of baking. In the crust region of the fifteen-minute fried samples, the resistant starch was 4.2 % of the total starch. They suggested that the formation of amylose-lipid complex caused lowering of resistant starch in crust region of samples after 15 min of frying. Because amylose led to the formation of resistant starch, while the complex of amylose and lipid caused a reduction of resistant starch. Therefore, they confirmed the formation of amylose-lipid complex with iodimetric determination of amylose or blue value and found that the crust region had less blue value than the core region. This was due to the contact of crust region with oil, resulting in the formation of amylose-lipid complex. Moreover, different starches with various amylose contents had slightly differed in blue value, causing the formation of amylose-lipid complex occurred only in the crust region. These results suggested that the formation of amylose-lipid complex presented in the crust region of a fried sample. Thus the amylose content in raw materials did not reflect amylose-lipid complex during frying (Pinthus *et al.*, 1998).

As mention aboved, the rationale of this study proposed that the solid foam structure is generated from air bubble dispersed in starch-protein matrix. Therefore, controlling starch-protein matrix of rice sheets before frying can lead to the formation of various sizes of air cells, which affected oil absorption. The viscoelastic properties of starch-protein matrix can be manipulated by controlling the degree of starch gelatinization and interaction with proteins by adjusted flour composition and using hydrocolloids.

MATERIALS AND METHODS

Materials

1. Raw material

1.1 Rice flour (RF) (Erawan, Cho Heng Rice Vermicelli Factory Co., Ltd., Thailand) containing amylose content of 29.75 % d.b.

1.2 Waxy rice flour (WF) (Erawan, Cho Heng Rice Vermicelli Factory Co., Ltd., Thailand) containing amylose content of 4.13 % d.b.

1.3 Rice bran oil (King, Thai Edible Oil Co., Ltd., Thailand)

1.4 Sodium alginate (Algogel[®] 6021, Food grade, lot no. 3700801, Degussa Texturant Systems, Degussa Texturant Systems France SAS, Boulogne-Billancourt, France)

1.5 Methylcellulose (MC) (TIC PRETESTED[®] TICACEL[®] HV Powder, Food grade, lot no. 10172, TIC gums, TIC gums, Inc., Belcamp, USA)

2. Chemical reagent

2.1 De-proteinization of flour

2.1.1 Bromelain (EC no. 3.4.22.32; Analytical grade, lot no. 025K1482, Sigma, Sigma-Aldrich, Inc., Saint Louis, USA)

2.1.2 Sodium azide (NaN₃; Analytical grade, lot no. 017K0136, Sigma-Aldrich, Sigma-Aldrich, Inc., Saint Louis, USA)

2.2 Colorimetric determination of amylose

2.2.1 Iodine (I_2 ; Analytical grade, Merck, Merck KGaA, Darmstadt, Germany)

2.2.2 Methanol (CH_3OH ; Analytical grade, Carlo Erba Reagents, Carlo Erba Reagenti S.P.A., Rodano, Italy)

2.2.3 Potassium iodide (KI; Analytical grade, Merck, Merck KGaA, Darmstadt, Germany)

2.2.4 Potato amylose ($(C_6H_{10}O_5)_n$; lot no. 084K3808, Sigma, Sigma-Aldrich, Inc., Saint Louis, USA)

2.2.5 Sodium hydroxide (NaOH; Analytical grade, Merck, Merck KGaA, Darmstadt, Germany)

2.2.6 Trichloroacetic acid (TCA) ($C_2HCl_3O_2$; Analytical grade, POCH, POCH S.A., Gliwice, Poland)

2.3 Protein determination

2.3.1 Boric acid (H_3BO_3 ; Analytical grade, Merck, Merck KGaA, Darmstadt, Germany)

2.3.2 Bromocresol green ($C_{21}H_{14}Br_4O_5S$; Analytical grade, LABCHEM, Ajax Finechem Pty Ltd, Auckland, New Zealand)

2.3.3 Copper sulfate ($CuSO_4 \cdot 5H_2O$; Analytical grade, Fisher Chemicals, Fisher Scientific UK Limited, Loughborough, UK)

2.3.4 Methyl red ($C_{15}H_{15}N_3O_2$; Analytical grade, Panreac, Panreac Quimica S.A., Barcelona, Spain)

2.3.5 Potassium sulfate (K_2SO_4 ; Analytical grade, Merck, Merck KGaA, Darmstadt, Germany)

2.3.6 Sodium hydroxide (NaOH; Commercial grade, THASCO, THASCO Chemical Co., Ltd., Thailand)

2.3.7 Sulfuric acid (H_2SO_4 ; Analytical grade, Mallinckrodt Chemicals, Mallinckrodt Baker, Inc., Phillipsburg, USA)

2.4 Fat determination

2.4.1 Petroleum ether (C_6H_6 ; Analytical grade, Mallinckrodt Chemicals, Mallinckrodt Baker, Inc., Phillipsburg, USA)

2.5 Sodium dodecyl sulfate-polyacrylamide gel electrophoresis (SDS-PAGE)

2.5.1 Acetic acid (CH_3COOH ; Analytical grade, J.T.Baker, Mallinckrodt Baker, Inc., Phillipsburg, USA)

2.5.2 Acrylamide-PAGE ($CH_2:CHCONH_2$; Ultrapure, PlusOne, Amersham Biosciences AB, Uppsala, Sweden)

2.5.3 Ammonium persulfate (APS) ($(NH_4)_2S_2O_8$; Ultrapure, BIO-RAD, Bio-Rad Laboratories, Hercules, USA)

2.5.4 Bromophenol blue sodium salt ($C_{19}H_9Br_4NaO_5S$; Ultrapure, usb, USB corporation, Cleveland, USA)

2.5.5 Coomassie brilliant blue (Coomassie[®] brilliant blue R-250) ($C_{45}H_{44}N_3O_7S_2Na$; Ultrapure, BIO-RAD, Bio-Rad Laboratories, Hercules, USA)

2.5.6 Glycerol ($CH_2OHCHOHCH_2OH$; Analytical grade, Carlo Erba Reagents, Carlo Erba Reagenti S.P.A., Rodano, Italy)

2.5.7 Glycine (NH_2CH_2COOH ; Ultrapure, BIO-RAD, Bio-Rad Laboratories, Hercules, USA)

2.5.8 Hydrochloric acid (HCl; Analytical grade, Merck, Merck KGaA, Darmstadt, Germany)

2.5.9 2-Mercaptoethanol ($HSCH_2CH_2OH$; Ultrapure, BIO-RAD, Bio-Rad Laboratories, Hercules, USA)

2.5.10 Methanol (CH_3OH ; Analytical grade, Carlo Erba Reagents, Carlo Erba Reagenti S.P.A., Rodano, Italy)

2.5.11 N,N'-Methylenebisacrylamide ($((CH_2:CHCONH)_2CH_2$; Ultrapure, PlusOne, GE Healthcare Bio-sciences AB, Uppsala, Sweden)

2.5.12 Protein standard (RPN800; Full-Range Rainbow[™]Molecular Weight Markers (10-250 kDa), lot no. 72, Amersham, GE Healthcare UK Limited, Little Chalfont, UK)

2.5.13 Sodium dodecyl sulphate (SDS) ($C_{12}H_{25}OSO_3Na$; Ultrapure, PlusOne, Amersham Biosciences AB, Uppsala, Sweden)

2.5.14 N, N, N', N'-Tetramethylethylenediamine (TEMED) ($C_6H_{16}N_2$; Ultrapure, usb, USB corporation, Cleveland, USA)

2.5.15 Tris (Tris [hydroxymethyl] aminomethane) ($NH_2C(CH_2OH)_3$; Ultrapure, usb, USB corporation, Cleveland, USA)

2.6 Confocal laser scanning microscopy (CLSM)

2.6.1 Rhodamine B ($C_{29}H_{30}ClN_3O_3S$; For fluorescence, Fluka, Sigma-Aldrich, Inc., Buchs, Switzerland)

3. Apparatus

3.1 De-proteinization of flour

3.1.1 Hot air oven (Mettler, model ULM400, Mettler GmbH + Co. KG, Schwabach, Germany)

3.1.2 Incubator shaker (Innova, model InnovaTM4340, New Brunswick Scientific Co., Inc., Edison, USA)

3.1.3 pH meter (OMEGA, model PHB-62, Omega Engineering, Inc., Stamford, USA)

3.1.4 Refrigerated centrifuge (DuPont / Sorvall[®] Instruments, model RC-28S, DuPont Company, Newtown, USA)

3.1.5 Weight balance (OHAUS, model TP4KS, Ohaus Corporation, Florham park, USA)

3.2 Sample preparation

3.2.1 Centrifuge (Chonracha Co., Ltd., Thailand)

3.2.2 Freezer (SANYO, model SR-F215A SWS, Sanyo Universal Electric Plc, Thailand)

3.2.3 Fryer (Fritel Professional 35, model 48/49, J. van Ratingen nv, Hasselt, Belgium)

3.2.4 Hot air oven (Kasetsart University, Thailand)

3.2.5 Steamer (Hi sonic, model HS-639, GW Revolution Co., Ltd., Thailand)

3.2.6 Weight balance (OHAUS, model TP4KS, Ohaus Corporation, Florham park, USA)

3.3 Application methods of hydrocolloids

3.3.1 Hot air oven (Mettler, model ULM400, Mettler GmbH + Co. KG, Schwabach, Germany)

3.4 Analytical methods

3.4.1 Centrifuge (Heraeus Biofuge primo, model D 37520 Osterode, Kendro Laboratory Products GmbH, Hanau, Germany)

3.4.2 Confocal laser scanning microscope (CLSM) (Zeiss, model Axio Imager MI; He/Ne laser acquired with LSM 5 PAS-CAL program, Carl Zeiss Pte. Ltd., Jena, Germany)

3.4.3 Electrophoresis cell (BIO-RAD, model Mini-PROTEAN 3, Bio-Rad Laboratories, Inc., Hercules, USA)

3.4.4 Hot air oven (Mettler, model ULM400, Mettler GmbH + Co. KG, Schwabach, Germany)

3.4.5 Lipid analytical apparatus (Tecator, Tecator AB, Höganäs, Sweden) (Appendix A)

3.4.6 Microcentrifuge (Labnet, model Spectrafuge 16M, Labnet International, Inc., Edison, USA)

3.4.7 Muffle furnace (Gallenkamp, model FSE-261-210D, Weiss-Gallenkamp, Loughborough, UK)

3.4.8 Protein analytical apparatus (BÜCHI, BÜCHI Labortechnik AG, Flawil, Switzerland) (Appendix A)

3.4.9 Rapid Visco Analyzer (RVA) (Newport Scientific, model RVA-4, Newport Scientific Pty. Ltd., Warriewood, Australia)

3.4.10 Stereo microscope (Leica Microsystems, model Leica S8 APO, Leica Microsystems Ltd, Wetzlar, Germany) and Digital image program (Dewinter, Licensed Version 4.1, Dewinter Software Inc., New Delhi, India)

3.4.11 UV-visible spectrophotometer (Spectronic, model Genesys 10-S, Thermo Electron Corporation, Madison, USA)

3.4.12 Vortex mixer (Vortex-Genie 2, model G-560E, Scientific industries, Inc., Bohemia, USA)

3.4.13 Water bath (Mettler, model OB14, Mettler GmbH + Co. KG, Schwabach, Germany)

3.4.14 Weight balance (Scale Tech, model SPB31, Scaltec Instruments GmbH, Göttingen, Germany)

Methods

1. Experimental preparation

1.1 Preparation of de-proteinized flour by bromelain

Low protein rice flour (LPRF) and low protein waxy rice flour (LPWF) were produced by hydrolyzing the flour by bromelain. Solution was composed of 1:10 (w/v) ratio of flour to solution with 1% (w/v) of bromelain. The solution was added with 0.02 % (w/v) sodium azide and adjusted to pH 6.5. The flour suspension was incubated at 30°C for 19 hr; the supernatant was discarded after centrifugation at 5000 rpm at 20°C for 5 min. The protein was washed out with distilled water after centrifugation at 5000 rpm at 20°C for 5 min, five times. Low protein flours were dried at 40°C for 24 hr in a hot air oven.

1.2 Preparation of rice sheet and rice cracker

Rice sheet samples were prepared by dispersing flour at 40 % (w/w) in tap water and poured onto a tray to acquire the thickness of 2 mm, steamed for 3 min, cooled down at room temperature (25°C) and frozen at -20°C for 14 hr. The sheets were cut into 10×10×2 mm, dried at 45°C for 3 hr and deep-fat fried in rice bran oil at 170°C for 15 s to produce rice cracker. Rice crackers were drained through screen for 1 min and oil-sorbed by blotting paper for 1 min, and then centrifuged at 1166 rpm for 5 min to remove excess oil.

1.3 Application methods of hydrocolloids

The hydrocolloids; i.e. sodium alginate and methylcellulose, were applied by two different methods. The first method was achieved by mixing sodium alginate or methylcellulose solution into flour during rice sheet preparation to obtain 0.1 % (w/v) of hydrocolloids in final flour slurries. Coating with hydrocolloids was carried

out by dipping the dried rice sheet in 1% (w/v) solution of sodium alginate or methylcellulose. The coated rice sheets were dried with hot air oven at 80°C for 50 min to produce coated rice sheets.

2. Analytical Methods

2.1 Proximate analysis

Commercially available RF and WF purchased from a local supermarket and de-proteinized flour prepared as described above were proximately analyzed for moisture, protein, lipid and ash contents (Appendix A).

2.2 Electrophoresis

Proteins from RF, WF, LPRF and LPWF (0.0057 mg protein), in the absence and presence of β -mercaptoethanol, were characterized for protein molecular weight profiles by SDS-PAGE. Protein extracts were prepared by suspending the flours in sample buffer containing 12.5 % of 0.5 M Tris-HCl (pH 6.8), 10 % glycerol, 2 % SDS, 5 % 2-mercaptoethanol and 0.05 % bromophenol blue. The suspensions were boiled for 20 min with intermittent vortex mixing and 10 μ l of supernatants were loaded into wells of polyacrylamide slab gel consisting of 4 % stacking and 15 % separating gels. Gels were run at constant voltage of 150 V for 1 hr. Molecular weight of storage proteins were determined by comparing with full-range rainbow molecular weight markers (10-250 kDa) as molecular weight standards.

2.3 Pasting properties

The pasting profiles of RF, WF, LPRF and LPWF were studied by Rapid Visco Analyser (RVA) (Appendix A).

2.4 Moisture and oil contents

Rice sheets and rice crackers were ground into small pieces and analyzed for moisture and oil contents (Appendix A).

2.5 Amylose content

RF and WF were analyzed for amylose by colorimetric quantitation. Flours (10-20 mg) were mixed with 5 ml of 85 % methanol, heated at 60°C for 15 min, discarded supernatant and collected the solid. This process was repeated twice to remove lipids in sample. Lipid-free samples were solubilized with 2 ml of 0.4 N NaOH and 4 ml of distilled water, and heated at 95°C for 30 min. The solubilized solutions (0.1 ml) were added into 5 ml of 0.5% TCA and mixed immediately with 0.05 ml of 0.01 N I₂-KI solution. The absorbance of sample was read at 620 nm (Appendix A).

2.6 Expansion for width and thickness

The width and thickness of rice crackers were measured using a vernier caliper. Measurement was performed for 20 readings for each treatment. % Expansion for width and thickness were calculated as follows:

$$\% \text{ Expansion} = \frac{\text{Dimension after frying} - \text{Dimension before frying}}{\text{Dimension before frying}} \times 100$$

2.7 Stereo microscope

The size distribution of air cells in rice crackers were observed under the stereo microscope using Dewinter software. The diameter (µm) of 10 air cells per field were measured. The data on the size of air cell were collected in 10 fields. All data were interpreted into histogram of size distribution of air cell.

2.8 Confocal Laser Scanning Microscopy (CLSM)

Rice sheet was stained with rhodamine B solution (0.01 % in 95 % ethanol) to label protein and incubated for 5 min. Sample was loaded into slide well and observed for a location of fluorescent-labelled protein using a Confocal Laser Scanning Microscope (CLSM) using method described by Hongsprabhas *et al.* (2007).

3. Statistical Analysis

The data were analyzed by two tailed t-test and the Analysis of Variance (ANOVA) with significance at $p < 0.05$. Significant differences among mean values were determined by Duncan's multiple range test. All statistical analyses were performed using the SPSS Software Version 12.

RESULTS AND DISCUSSION

1. Effect of flour composition

De-proteinization by bromelain reduced more than 50 % of protein content ($p<0.05$); i.e., to 2.88 % in LPRF and 2.75 % in LPWF compared with 7.32 % in RF and 6.08 % in WF, respectively (Table 1). This result probably due to the fact that bromelain hydrolyzed the peptide bonds of proteins, resulting in peptides and amino acids (Whitaker, 1972), which is more water-soluble. In addition, de-proteinization step also lowered lipid and ash contents ($p<0.05$). This was probably because most of the lipids in endosperm are associated with protein bodies (Godber and Juliano, 2004), de-proteinization could lead to the loss of lipid during washing. Phosphorus and potassium are the most abundant minerals in milled rice (Champagne *et al.*, 2004). They are highly water soluble (Miller, 1996). Therefore, the reduction in lipid and ash contents apart from protein could occur after washing for 5 times in de-proteinization process.

Table 1 Composition of rice flour and waxy rice flour (g/100 g wb).

Flour type	Moisture	Protein	Lipid	Ash
RF	12.22 ^a ±0.16	7.32 ^a ±0.12	0.24 ^a ±0.04	0.25 ^a ±0.01
LPRF	12.03 ^a ±0.17	2.88 ^c ±0.02	0.09 ^b ±0.04	0.16 ^c ±0.01
WF	12.38 ^a ±0.14	6.08 ^b ±0.14	0.29 ^a ±0.03	0.20 ^b ±0.00
LPWF	11.53 ^a ±1.07	2.75 ^c ±0.06	0.07 ^b ±0.05	0.08 ^d ±0.01

Means in the same column followed by different superscript are significantly different ($p<0.05$).

RF = rice flour; WF = waxy rice flour; LPRF = low protein rice flour and LPWF = low protein waxy rice flour

De-proteinization of flours by bromelain also altered the RVA pasting profiles (Table 2). The lowering of protein content increased peak viscosity but decreased final viscosity of RF slurries ($p<0.05$). Moreover, the peak time required to reach peak viscosity in RF slurries was shortened when the protein was reduced ($p<0.05$). This was probably due to the fact that protein retarded swollen rice starch granules and formed three-dimensional networks after denaturation under thermal process. Therefore, reduction of protein content allow rice starch granule to swell faster, leading to higher peak viscosity. In contrast, peak viscosity in WF slurries was decreased when the protein content was lowered ($p<0.05$). This suggested that the involvement of protein was not only in retardation of swelling of starch granule but also in the bulk viscosity of the easily swollen waxy rice granules. Lowering the protein content of WF also gave the paste with less shear-resistant at high temperature, observed as lower holding strength ($p<0.05$). The final viscosity of both RF and WF were lowered when the flours were de-proteinized ($p<0.05$) although amylose and amylopectin in one of each remained unchanged. This was probably because protein stabilized swollen rice starch granules and formed three-dimensional networks after denaturation under thermal process. Overall, de-proteinization by bromelain lowered final viscosity of both RF and WF paste.

RF contained 29.75 % amylose while WF was composed of 4.13 % amylose ($p<0.05$) (Table 3). This study suggested that not only amylose content, but also protein content, that played significant roles in RVA pasting profile.

Table 2 RVA pasting profiles of rice flour and waxy rice flour containing different protein contents.

Flour type	RVA pasting parameters				
	Pasting temperature (°C)	Peak time (min)	Peak viscosity (mPa.s)	Holding strength (mPa.s)	Final viscosity (mPa.s)
RF	50.17 ^a ±0.05	6.50 ^a ±0.00	3240.25 ^c ±85.21	2495.50 ^a ±89.80	5034.50 ^a ±43.84
LPRF	50.40 ^a ±0.28	6.30 ^b ±0.04	3492.25 ^b ±74.60	2469.00 ^a ±1.41	4582.50 ^b ±108.19
WF	53.21 ^a ±3.64	3.73 ^c ±0.00	4857.75 ^a ±34.29	2551.50 ^a ±31.82	3094.00 ^c ±50.91
LPWF	50.67 ^a ±0.62	3.69 ^c ±0.02	3654.25 ^b ±7.42	1897.75 ^b ±13.08	2173.00 ^d ±26.87

Means in the same column followed by different superscript are significantly different ($p < 0.05$).

RF = rice flour; WF = waxy rice flour; LPRF = low protein rice flour and LPWF = low protein waxy rice flour

Table 3 Amylose content of rice flour and waxy rice flour (g/100 g db).

Flour type	Amylose content (%)
RF	29.75 ^a ±1.60
WF	4.13 ^b ±0.37

Means in the same column followed by different superscript are significantly different ($p < 0.05$).

RF = rice flour and WF = waxy rice flour

The reduction of protein content in RF and WF increased the average air cell diameter (Figure 12 and 13). In rice crackers made of LPRF (Figures 12b and 13b), the lower protein content allowed the air cell to expand to a larger size, compared to the small size of air cell between 1-600 μm in diameter in rice cracker made of RF (Figure 12a and 13a). Rice cracker made of LPRF had large air cell size between 301-1200 μm in diameter (Figure 12b and 13b). Rice cracker made of RF:WF and LPRF:LPWF at the ratio of 0.7:0.3, lowering the protein content also allowed the air cell to expand to a larger size (Figures 12c, 12d, 13c and 13d). Small air cell size was found in rice cracker made of RF:WF at the ratio of 0.7:0.3 with the size ranged between 301-1500 μm in diameter (Figure 12c and 13c). Rice cracker made of LPRF:LPWF at the ratio of 0.7:0.3 had large size of air cell between 301-1800 μm in diameter (Figure 12d and 13d). These were probably due to the different amylose content of the composite and low final viscosity of cooked rice flour pastes when WF or LPWF was included. The results suggested that the amylose content, together with protein content, played significant role in controlling the expansion of the air cell during frying.

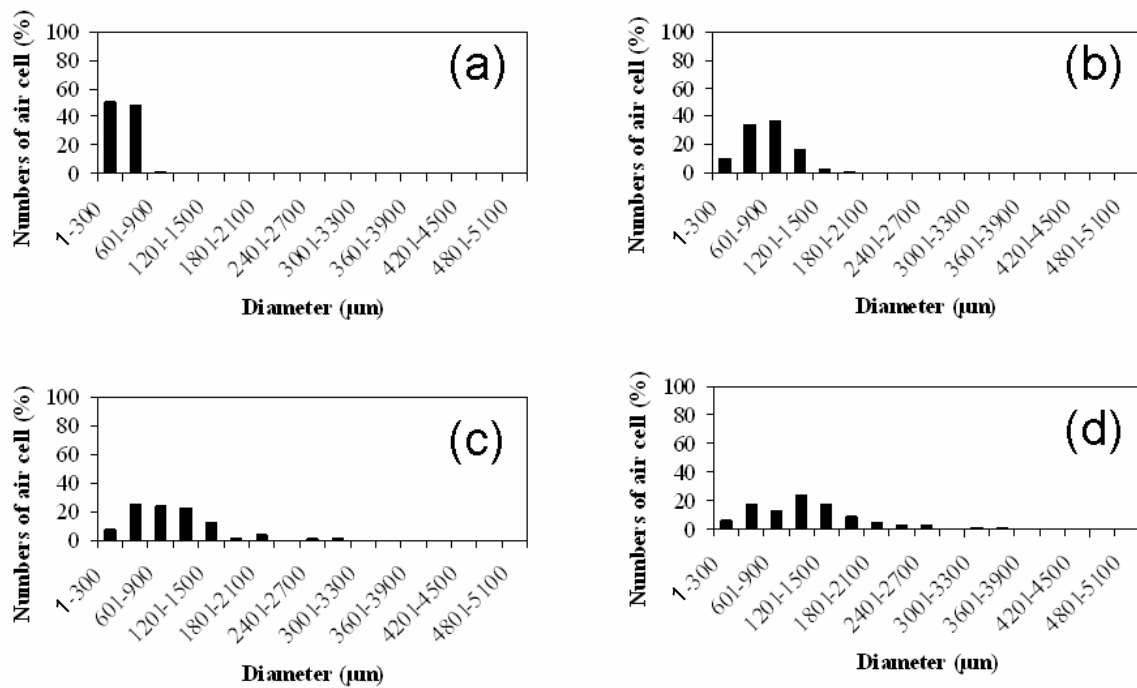


Figure 12 Effect of protein content of rice flour (RF) and waxy rice flour (WF) on size distribution of air cells in rice crackers; a = RF; b = LPRF; c = RF:WF (0.7:0.3) and d = LPRF:LPWF (0.7:0.3).

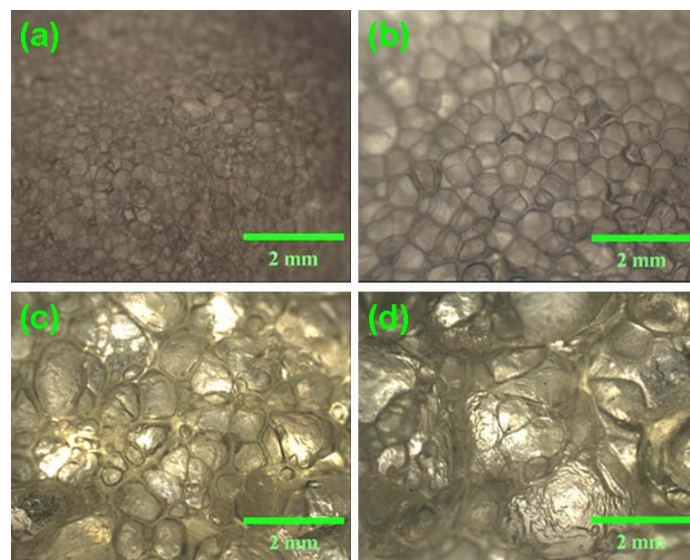


Figure 13 Effect of protein content of rice flour (RF) and waxy rice flour (WF) on microstructure in rice crackers; a = RF; b = LPRF; c = RF:WF (0.7:0.3) and d = LPRF:LPWF (0.7:0.3). Scale bar was 2 mm.

However, the larger size of the air cells, when the protein content was lowered, did not affect oil absorption of the rice cracker ($p \geq 0.05$) (Table 4). The rice crackers made of RF had similar oil absorption as the ones made of LPRF, which were around 16-22 % ($p \geq 0.05$). The crackers made of RF:WF and LPRF:LPWF at the ratio of 0.7:0.3, although showed similar oil absorption, had tendency of a higher oil uptake. Protein controlled the size of air cell with limit capability. De-proteinization led to larger air cell size, particularly the thickness expansion of the cracker. Lowering of protein content by bromelain hydrolysis made LPRF cracker expand to the highest ($p < 0.05$) compared with RF cracker. The expansion of thickness of rice cracker made of LPRF:LPWF at the ratio of 0.7:0.3 was not significantly changed when the protein content was lowered ($p \geq 0.05$) compared with RF:WF at the ratio of 0.7:0.3 cracker.

Use of rice flour composite in this study alters the ratio between amylose and amylopectin while maintaining protein content. It was found that the low final viscosity in WF and LPWF could lead to less retrogradation of the composite. This caused less tight barrier that prevented expansion of the air cell. These results indicated that amylose:amylopectin ratio also affected the size of air cell and oil absorption. Apart from physical characteristics such as size of air cell and expansion, the effect of ingredient interactions on oil absorption should be considered.

Table 4 Effect of protein content of rice flour and waxy rice flour on water content, oil absorption and expansion in rice crackers.

Flour type	Moisture content of rice sheet before frying (g/100 g wb)	Moisture content of rice cracker after frying (g/100 g wb)	Oil content of rice cracker after frying (g/100 g db)	Expansion (%)	
				Width	Thickness
RF	11.50 ^a ±1.80	5.63 ^a ±0.59	15.70 ^a ±7.30	32.69 ^a ±11.93	137.44 ^b ±11.01
LPRF	11.81 ^a ±1.61	5.41 ^a ±1.27	22.17 ^a ±7.12	51.45 ^a ±5.92	190.32 ^a ±4.39
RF:WF	11.49 ^a ±1.46	4.43 ^a ±1.25	27.59 ^a ±9.42	45.53 ^a ±21.43	150.77 ^b ±1.38
LPRF:LPWF	11.98 ^a ±1.56	3.93 ^a ±1.09	34.02 ^a ±12.66	49.92 ^a ±8.20	167.53 ^{ab} ±23.49

Means in the same column followed by different superscript are significantly different ($p < 0.05$).

RF = rice flour; LPRF = low protein rice flour; RF:WF = 0.7:0.3 rice flour to waxy rice flour ratio and LPRF:LPWF = 0.7:0.3 low protein rice flour to low protein waxy rice flour ratio.

The proteins in flours were characterized by SDS-PAGE for storage rice proteins (Figure 14). Lane 1 and 2 were RF and WF, respectively, in the absence of β -mercaptoethanol. Storage proteins in RF and WF had molecular weight (MW) of more than 250 kDa, 105 kDa, 50 kDa, between 35-50 kDa, between 15-25 kDa and between 10-14.3 kDa. Storage proteins in RF and WF were slightly different in terms of the proteins with the MW of 50 kDa which was presented only in RF. Lane 3 and 4 were LPRF and LPWF, respectively, in the absence of β -mercaptoethanol. De-proteinization by bromelain for 19 hours showed no difference in polypeptides with high MW. However, there was disappearance of the proteins with MW between 15-25 kDa and proteins with MW 10 kDa appeared. This indicated that bromelain could not hydrolyze all of the storage rice proteins, but it hydrolyzed the proteins to the lower MW. Although bromelain could only slightly change in proteins pattern, it

could help reducing protein content (Table 1). The addition of β -mercaptoethanol to reduce disulfide bonds illustrates that proteins were linked by disulfide bonds (Lane 5-8). As a result, de-proteinization by bromelain hydrolysis increased the air cell size not only by the reduction of protein content (Table 1) but also shortening the polypeptide chains.

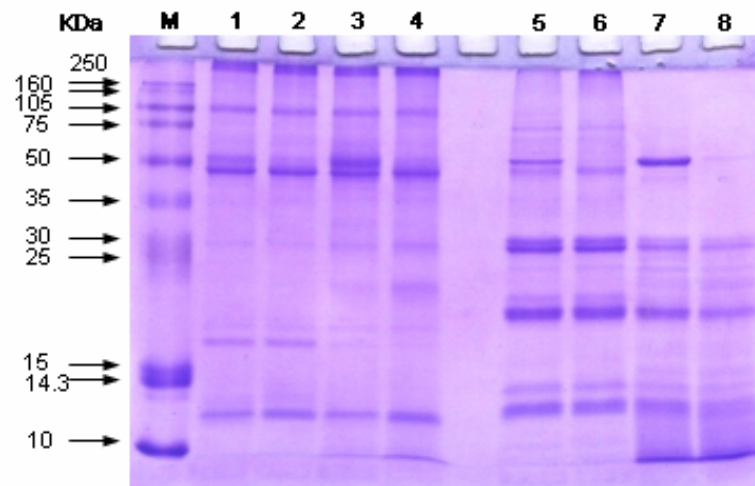


Figure 14 SDS-PAGE profiles of storage rice proteins in the absence (lane 1-4) and presence (lane 5-8) of β -mercaptoethanol. Lane 1, 5 = RF; Lane 2, 6 = WF; Lane 3, 7 = LPRF and Lane 4, 8 = LPWF. The molecular weight standards = lane M.

The composite containing RF to WF at the ratio of 0.7:0.3 was investigated to understand the roles of amylose:amylopectin ratio on pasting characteristics, air cell size distribution and microstructure. When the WF content was increased in the mixed paste, it altered pasting profile, especially decreasing in final viscosity ($p < 0.05$) (Table 5). Thus, the viscoelastic properties of starch-protein matrix in rice sheet before frying may be different. Increasing the ratio of WF, which reduced amylose content and final viscosity, altered the size distribution of air cell to the larger size (Figure 15 and 16). Rice cracker with the highest ratio of WF had large size of air cell of between 301-1800 μm in diameter (Figure 15d and 16d), whereas rice cracker had small size of air cell of between 1-600 μm in diameter (Figure 15a and 16a).

Table 5 Effect of rice flour (RF) to waxy rice flour (WF) ratios on RVA pasting characteristics in flour composites.

RF:WF ratio	RVA pasting parameters				
	Pasting temperature (°C)	Peak time (min)	Peak viscosity (mPa.s)	Holding strength (mPa.s)	Final viscosity (mPa.s)
1.0:0.0	50.17 ^a ±0.05	6.50 ^a ±0.00	3240.25 ^b ±85.21	2495.50 ^a ±89.80	5034.50 ^a ±43.84
0.7:0.3	50.19 ^a ±0.08	6.37 ^b ±0.04	3610.25 ^a ±18.74	2788.00 ^a ±58.69	4566.50 ^b ±6.36

Means in the same column followed by different superscript are significantly different ($p < 0.05$).

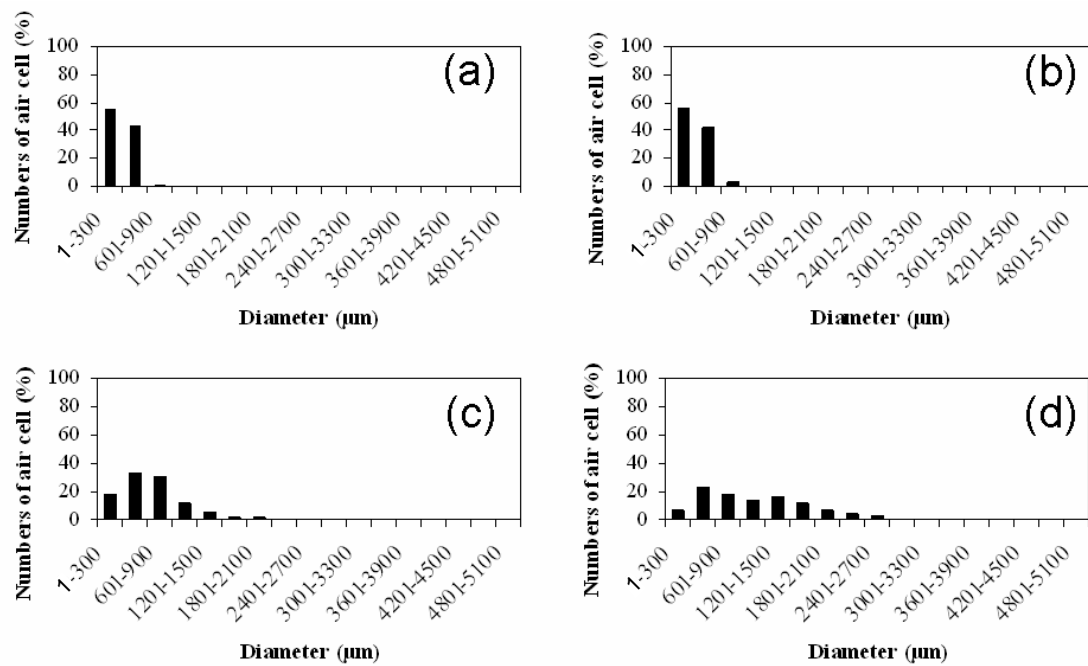


Figure 15 Effect of rice flour (RF) to waxy rice flour (WF) ratios on the size distribution of air cells in rice crackers. RF:WF ratios were (a) 1.0:0.0; (b) 0.9:0.1; (c) 0.8:0.2 and (d) 0.7:0.3.

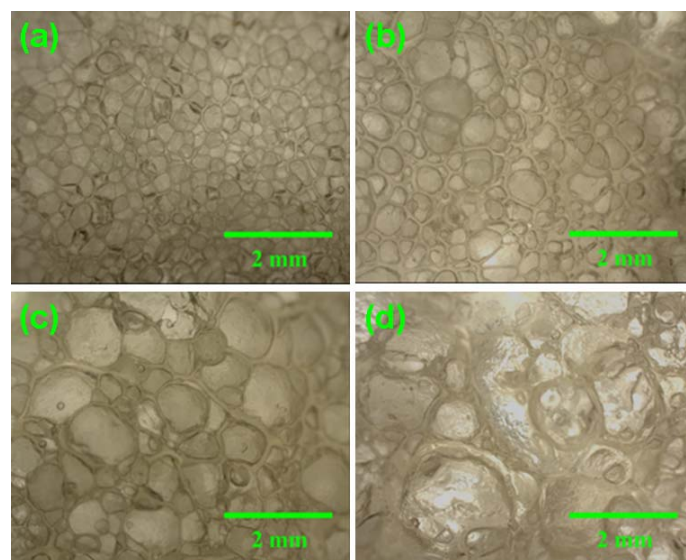


Figure 16 Effect of rice flour (RF) to waxy rice flour (WF) ratios on microstructure in rice crackers. RF: WF ratios were (a) 1.0:0.0; (b) 0.9:0.1; (c) 0.8:0.2 and (d) 0.7:0.3. Scale bar was 2 mm.

Moreover, the larger size of air cell generated by the highest ratio of WF led to the increase of oil absorption up to 40 % ($p < 0.05$) (Table 6) compared with RF cracker. This rice cracker with the highest ratio of WF had the highest expansion of width and thickness of up to 58 % and 191 %, respectively (Table 6) compared with those of RF cracker. These results showed that increasing WF ratio, which reduced amylose content, could increase the expansion of air cell size and oil absorption. This was probably due to weaker three-dimensional networks from lower degree of retrogradation, which resulted from the reduction of amylose content, could not withstand the expansion of water-vaporized pressure. This led to the larger size of air cell and an increase in oil absorption ($p < 0.05$) (Table 6) with size of air cell more than 1200 μm in diameter.

The effects of flour composition composed of different protein content and ratio of amylose:amylopectin showed that the lower protein content resulted in larger size of air cell and higher expansion of thickness, but it did not affect oil absorption. Moreover, decreasing in amylose content by increasing the ratio of WF, resulted in the larger size of air cell, increased oil absorption and expansion of width and thickness. These results showed that controlling starch-protein matrix of rice sheet before frying by manipulating protein content and the ratio of amylose:amylopectin could lead to various sizes of air cells. The size of air cells of more than 1200 μm in diameter affected the oil absorption in rice cracker. The oil absorption of rice cracker increased in accordance with the ratio of WF, which had lower amylose content than RF, though amylose cause formation of amylose-lipid complex when contact with oil during frying (Pinthus *et al.*, 1998). Therefore, oil absorption in rice cracker could slightly involve in the formation of amylose-lipid complex. The larger the size of air cells, the more oil absorption was found in rice cracker.

2. Effect of hydrocolloid application

The starch-protein matrix could be manipulated by the addition of hydrocolloids (Figure 17). Two types of hydrocolloids investigated were sodium alginate and methylcellulose. The addition of 0.1 % (w/v) sodium alginate in rice sheet (Figure 17c) showed that rice proteins, which fluoresced in red under CLSM, formed different distributions in the matrix compared to the microstructure of rice sheet prepared with only water (Figure 17a). This result was probably due to the negatively charge of carboxyl group on the high MW linear chain alginate (Trudso, 1991) repulsed the negatively charge of the rice protein in the system. Thus the aggregation of protein fractions was induced through phase separation. Methylcellulose addition at the concentration of 0.1 % (w/v) made scattered cluster of rice protein fractions under CLSM (Figure 17b). This was probably due to the fact that methylcellulose is a non-ionic cellulose derivative with methyl groups substituted (Williams and Phillips, 2000). Therefore, it was less effective in the induction of phase separation than did alginate. As a result, hydrocolloids were used to change the viscoelastic properties of protein-starch paste.

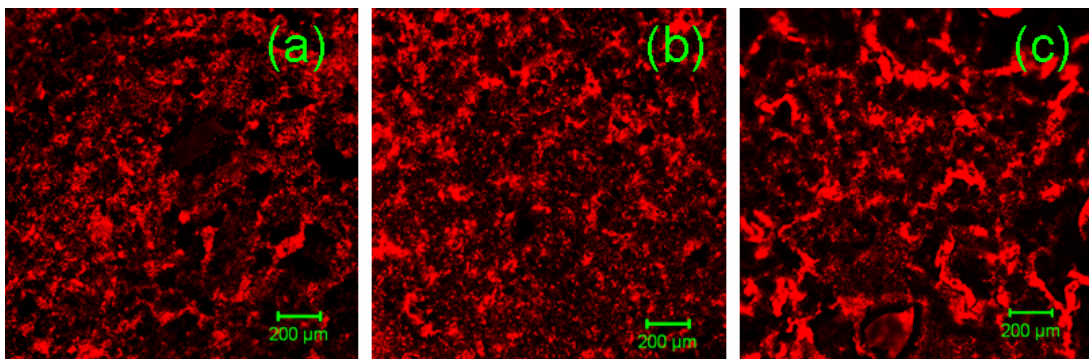


Figure 17 CLSM micrographs of rice sheets adding with 0.1 % (w/v) hydrocolloids; (a) water, (b) methylcellulose and (c) sodium alginate. Proteins were fluoresced in red staining by rhodamine B. Scale bar was 200 μm .

The effect of both hydrocolloids on oil absorption and expansion of RF:WF cracker with different ratios was shown in Table 6. Addition of 0.1 % (w/v) hydrocolloids during rice sheet preparation did not affect oil absorption and expansion of width and thickness in rice crackers ($p \geq 0.05$). The rice crackers added with 0.1 % (w/v) methylcellulose had similar oil absorption to rice crackers added with 0.1 % (w/v) sodium alginate, which was around 27-37% ($p \geq 0.05$). Moreover, expansions of width and thickness of rice cracker added with 0.1 % (w/v) methylcellulose and sodium alginate were not significantly different. The expansion was around 30-55 % and 124-172 % ($p \geq 0.05$), respectively.

Table 6 Effect of rice flour (RF) to waxy rice flour (WF) ratios and hydrocolloid addition on water content, oil absorption and expansion in rice crackers.

RF:WF ratio	Moisture content of rice sheet before frying (g/100 g wb)	Moisture content of rice cracker after frying (g/100 g wb)	Oil content of rice cracker after frying (g/100 g db)	Expansion (%)	
				Width	Thickness
Water					
1.0:0.0	12.38 ^a ±1.85	5.04 ^{ab} ±0.65	26.39 ^{bc} ±3.62	35.12 ^{cd} ±13.01	142.98 ^{ab} ±46.78
0.9:0.1	12.30 ^a ±1.97	5.13 ^a ±0.25	22.77 ^c ±3.45	27.35 ^d ±1.98	98.90 ^b ±54.26
0.8:0.2	11.27 ^a ±1.20	4.59 ^{abc} ±0.18	31.63 ^{abc} ±2.70	37.27 ^{bcd} ±3.38	98.08 ^b ±1.33
0.7:0.3	11.66 ^a ±0.57	4.02 ^{cd} ±0.13	40.03 ^a ±0.42	58.44 ^a ±1.03	191.37 ^a ±10.21
0.1 % (w/v) methylcellulose					
1.0:0.0	13.46 ^a ±0.98	4.39 ^{abcd} ±0.20	28.69 ^{abc} ±5.53	36.82 ^{bcd} ±14.08	131.04 ^{ab} ±17.20
0.9:0.1	12.94 ^a ±0.33	4.09 ^{cd} ±0.28	26.89 ^{bc} ±7.25	35.56 ^{cd} ±4.60	132.99 ^{ab} ±25.11
0.8:0.2	12.37 ^a ±1.41	3.90 ^{cd} ±0.18	35.01 ^{ab} ±6.75	43.16 ^{abcd} ±9.02	170.05 ^{ab} ±13.72
0.7:0.3	12.55 ^a ±0.65	4.02 ^{cd} ±0.25	36.75 ^{ab} ±3.33	55.08 ^{ab} ±7.52	123.53 ^{ab} ±3.59
0.1 % (w/v) sodium alginate					
1.0:0.0	13.36 ^a ±4.21	4.34 ^{abcd} ±0.28	28.84 ^{abc} ±1.32	40.73 ^{abcd} ±7.70	140.37 ^{ab} ±26.71
0.9:0.1	13.18 ^a ±4.06	4.23 ^{bcd} ±0.60	32.11 ^{abc} ±8.56	30.40 ^d ±8.79	170.38 ^{ab} ±72.18
0.8:0.2	11.93 ^a ±1.68	4.32 ^{abcd} ±0.48	31.19 ^{abc} ±2.27	40.75 ^{abcd} ±1.61	138.12 ^{ab} ±47.67
0.7:0.3	12.55 ^a ±1.11	3.58 ^d ±0.47	37.15 ^{ab} ±4.65	53.91 ^{abc} ±6.46	171.77 ^{ab} ±14.43

Means in the same column followed by different superscript are significantly different (p<0.05).

Addition of methylcellulose and sodium alginate at the concentration of 0.1 % (w/v) in RF:WF mixed cracker at the ratio of 0.7:0.3 did not affect the size of air cells compared with the sample prepared with water (Figure 18). Rice cracker prepared with water, methylcellulose and sodium alginate had large size of air cell between 301-1800 μm in diameter (Figure 18).

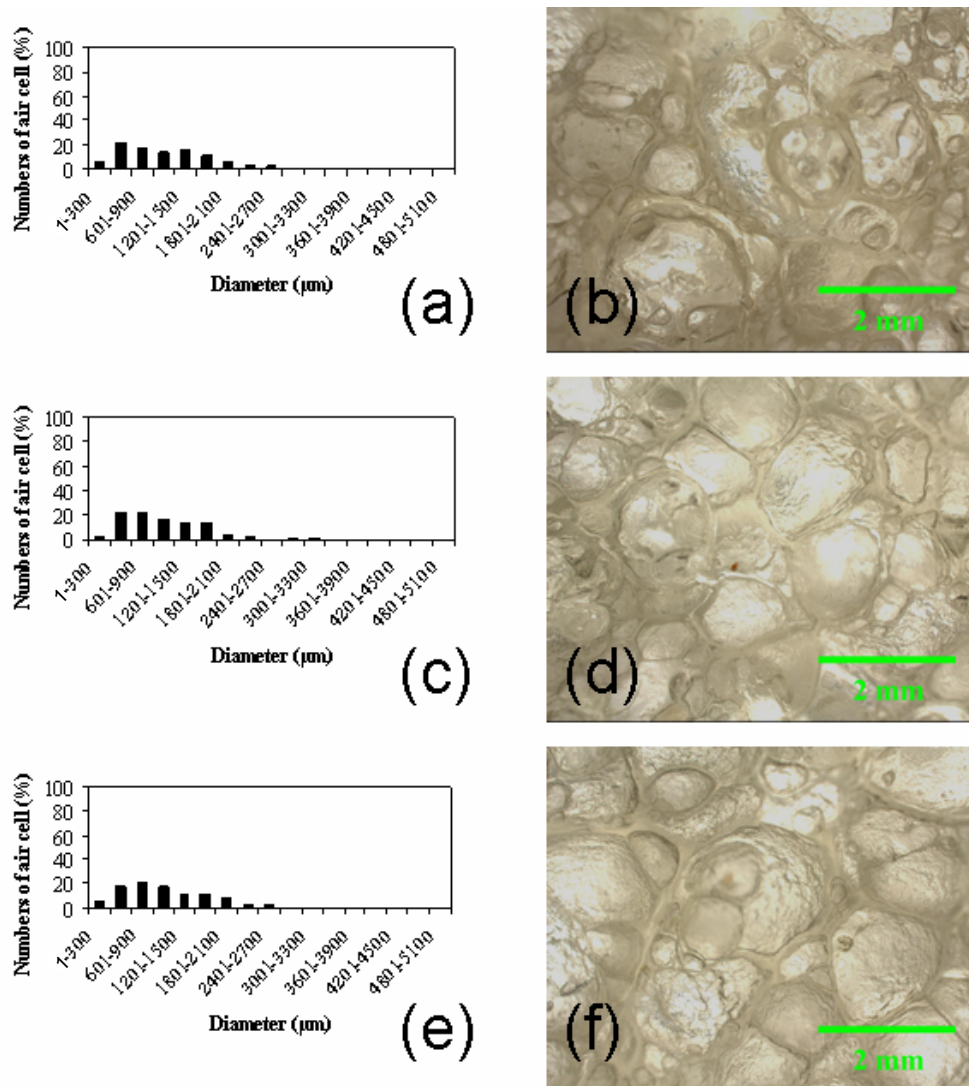


Figure 18 Effect of 0.1 % (w/v) hydrocolloids addition during rice sheet preparation on size distribution of air cells (a, c and e) and microstructure (b, d and f) in rice crackers (RF:WF ratio = 0.7:0.3). Rice crackers were mixed with water (a and b), methylcellulose (c and d) and sodium alginate (e and f). Scale bar was 2 mm.

At this stage, addition of 0.1 % (w/v) hydrocolloids during cooking did not alter the size distribution of air cells and oil absorption although it could generate different distribution of protein fraction in starch-protein matrix of rice sheet. These results were probably due to hydrocolloid led to decreasing in retrogradation of rice flour-hydrocolloid mixture (Hongsprabhas *et al.*, 2007). Therefore, coating of hydrocolloids on rice sheet before frying in rice cracker was studied. Rice crackers made of RF:WF at the ratio of 0.7:0.3 coated with methylcellulose and sodium alginate showed smaller size distribution of air cells compared with non-coated one (Figure 19). Rice crackers coated with methylcellulose and sodium alginate had small size of air cell of between 1-900 μm in diameter (Figure 19c, 19d, 19e and 19f); whereas the uncoated rice cracker had large air cell size between 301-1500 μm in diameter (Figure 19a and 19b).

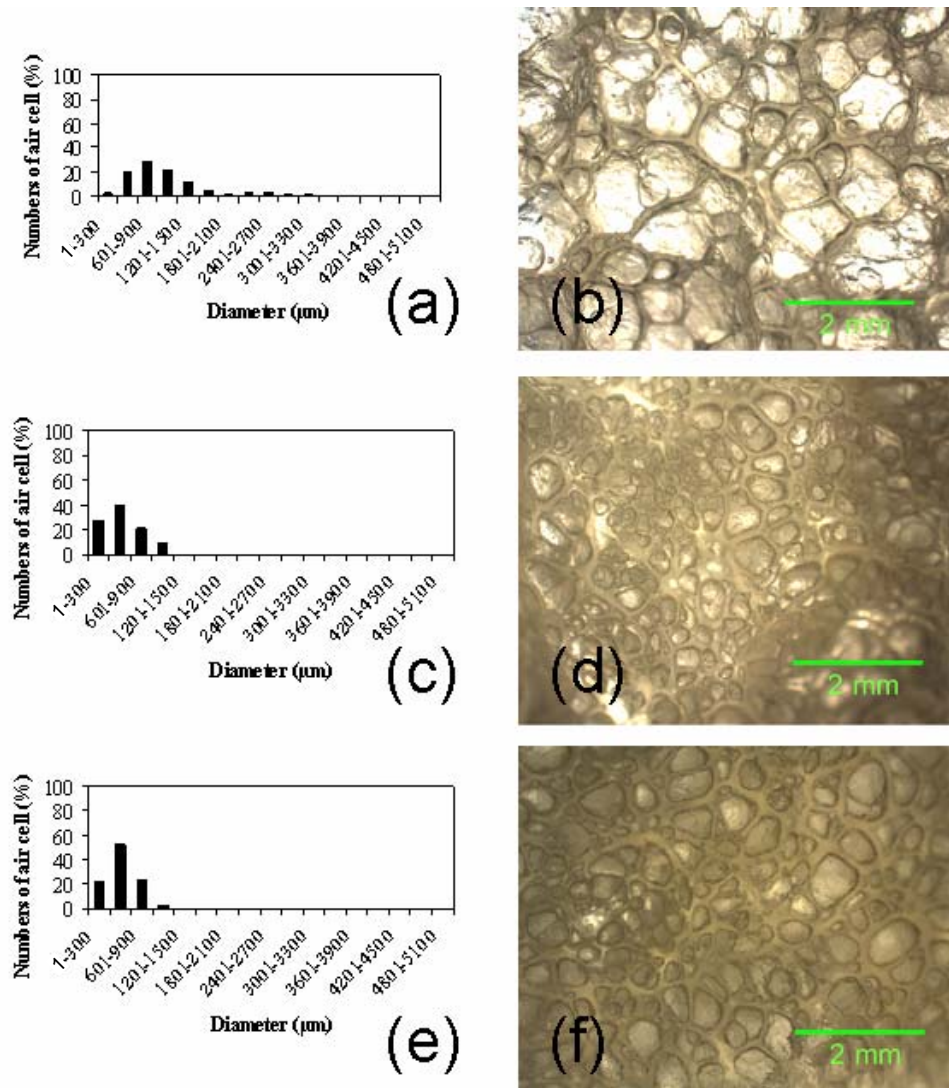


Figure 19 Effect of 1 % (w/v) hydrocolloids coating on rice sheet before frying on size distribution of air cells (a, c and e) and microstructure (b, d and f) in rice crackers (RF:WF ratio = 0.7:0.3). Rice crackers were coated with hydrocolloid (a and b), coating with methylcellulose (c and d) and sodium alginate (e and f). Scale bar was 2 mm.

Rice cracker made of RF:WF at the ratio of 0.7:0.3 coated with methylcellulose reduced the size of air cell, which led to the lower oil absorption and expansion of width compared with the non-coated sample ($p < 0.05$) (Table 7). Coated rice crackers had oil absorption around 15-16 %; while the uncoated one had oil absorption about 32 %. Furthermore, coating reduced expansion of width to more than 50 %. These were probably due to the fact that the hydrocolloids have hydrophilic property (Sanchez and Paquin, 1997). They acted like tight barrier to prevent oil absorption in rice cracker. Therefore, less oil was absorbed in rice crackers when coated with hydrocolloids.

Table 7 Effect of 1 % (w/v) hydrocolloid coating on water content, oil absorption and expansion in rice crackers (RF:WF ratio = 0.7:0.3).

Type of hydrocolloid	Moisture content of rice sheet before frying (g/100 g wb)	Moisture content of rice cracker after frying (g/100 g wb)	Oil content of rice cracker after frying (g/100 g db)	Expansion (%)	
				Width	Thickness
None	11.96 ^a ±0.36	4.54 ^a ±0.51	31.52 ^a ±7.92	44.19 ^a ±0.74	102.92 ^a ±14.95
Methyl cellulose	11.31 ^a ±0.19	5.43 ^a ±0.01	15.39 ^b ±1.88	15.97 ^b ±4.76	80.85 ^a ±21.73
Sodium alginate	11.26 ^a ±0.32	5.40 ^a ±0.99	15.81 ^{ab} ±3.03	21.03 ^{ab} ±12.77	120.08 ^a ±14.36

Means in the same column followed by different superscript are significantly different ($p < 0.05$).

CONCLUSION AND RECOMMENDATIONS

This study pointed out that viscoelastic properties of starch-protein matrix of rice sheet was controlled by the ratio of amylose:amylopectin and protein content. Rice cracker coated with 1% (w/v) methylcellulose led to the solid foam structure with small size distribution of air cells and low oil absorption. Furthermore, size of air cells larger than 1200 μm in diameter increased oil absorption in rice cracker. The understandings on the roles of flour composition and hydrocolloids on the size distribution of air cells and oil absorption might help formulating the low-fat fried products, resulting in the reduction of oil being used, lowering cost and increasing quality of final product for food industries. Moreover, the reduction of oil could respond the needs of health-concerned consumers in lowering of oil consumption and reducing the risk of chronic diseases.

LITERATURE CITED

- Aguilera, J.M. 1992. Generation of engineered structures in gels, pp. 387-421. *In* H.G. Schwartzberg and R.W. Hartel, eds. **Physical Chemistry of Foods**. Marcel Dekker, Inc., New York.
- Anonymous. 2006. **Tortilla chip**. Wikipedia, the Free Encyclopedia. Available Source: <http://www.en.wikipedia.org.htm>, December 28, 2006.
- AOAC. 1995. **Official Methods of Analysis**. 16th ed. Association of Official Analytical Chemists, Arlington, Virginia.
- Appelqvist, I.A.M. and M.R.M. Debet. 1997. Starch-biopolymer interactions: a review. **Food Rev. Int.** 13: 163-224.
- Bergman, C.J., K.R. Bhattacharya and K. Ohtsubo. 2004. Rice end-use quality analysis, pp. 415-472. *In* E.T. Champagne, ed. **Rice: Chemistry and Technology**. American Association of Cereal Chemists, Inc., Minnesota.
- Campbell, G.M. and E. Mougeot. 1999. Creation and characterization of aerated food products. **Trends Food Sci. Tech.** 10: 283-296.
- Champagne, E.T., D.F. Wood, B.O. Juliano and D.B. Bechtel. 2004. The rice grain and its gross composition, pp. 77-107. *In* E.T. Champagne, ed. **Rice: Chemistry and Technology**. American Association of Cereal Chemists, Inc., Minnesota.
- Chrastil, J. 1987. Improved colorimetric determination of amylose in starches or flours. **Carbohyd. Res.** 159: 154-158.

- Draget, K.I. 2000. Alginates, pp. 379-395. *In* G.O. Phillips and P.A. Williams, eds. **Handbook of Hydrocolloids**. Woodhead Publishing Limited, Cambridge.
- Eliasson, A.C. and M. Gudmundsson. 1996. Starch: physicochemical and functional aspects, pp. 431-503. *In* A. C. Eliasson, ed. **Carbohydrates in Food**. Marcel Dekker, Inc., New York.
- Fitzgerald, M. 2004. Starch, pp. 109-141. *In* E.T. Champagne, ed. **Rice: Chemistry and Technology**. American Association of Cereal Chemists, Inc., Minnesota.
- Garcia, M.A., C. Ferrero, N. Bertola, M. Martino and N. Zaritzky. 2002. Edible coatings from cellulose derivatives to reduce oil uptake in fried products. **Innov. Food Sci. & Emerg. Technol.** 3: 391-397.
- Godber, J.S. and B.O. Juliano. 2004. Rice lipids, pp. 163-190. *In* E.T. Champagne, ed. **Rice: Chemistry and Technology**. American Association of Cereal Chemists, Inc., Minnesota.
- Hamaker, B.R. 1994. The influence of rice protein on rice quality, pp. 177-194. *In* W.E. Marshall and J.I. Wadsworth, eds. **Rice Science and Technology**. Marcel Dekker, Inc., New York.
- Hongsprabhas, P., K. Israkarn and C. Rattanawattanapakit. 2007. Architectural changes of heated mungbean, rice and cassava starch granules: effects of hydrocolloids and protein-containing envelope. **Carb. Polym.** 67(4): 614-622.
- Ju, Z.Y., N.S. Hettiarachchy and N. Rath. 2001. Extraction, denaturation and hydrophobic properties of rice flour proteins. **J. Food Sci.** 66(2): 229-232.
- Kawas, M.L. and R.G. Moreira. 2001. Effect of degree of starch gelatinization on quality attributes of fried tortilla chips. **J. Food Sci.** 66: 300-306.

- Khalil, A.H. 1999. Quality of french fried potatoes as influenced by coating with hydrocolloids. **Food Chemistry**. 66: 201-208.
- Krokida, M.K., V. Oreopoulou and Z.B. Maroulis. 2000. Effect of frying conditions on shrinkage and porosity of fried potatoes. **J. Food Eng.** 43: 147-154.
- Mallikarjunan, P., M.S. Chinnan, V.M. Balasubramaniam and R.D. Phillips. 1997. Edible coatings for deep-fat frying of starchy products. **LWT-Food Sci. Technol.** 30: 709-714.
- Mellema, M. 2003. Mechanism and reduction of fat uptake in deep-fat fried foods. **Trends Food Sci. Technol.** 14: 364-373.
- Miller, D.D. 1996. Minerals, pp. 617-649. *In* O.R. Fennema, ed. **Food Chemistry**. 3rd ed. Marcel Dekker, Inc., New York.
- Moriera, R.G., J.E. Palau and X. Sun. 1995. Deep-fat frying of tortilla chips: an engineering approach. **Food Technol.** 49(4): 146-150.
- Moreira, R.G., X. Sun and Y. Chen. 1997. Factor affecting oil uptake in tortilla chips in deep-fat frying. **J. Food Eng.** 31: 485-498.
- Moyano, P.C. and F. Pedreschi. 2006. Kinetics of oil uptake during frying of potato slices: effect of pre-treatments. **LWT - Food Science and Technology**. 39: 285-291.
- Murphy, P. 2000. Starch, pp. 41-65. *In* G.O. Phillips and P.A. Williams, eds. **Handbook of Hydrocolloids**. Woodhead Publishing Limited, Cambridge.

- Murray, J.C.F. 2000. Cellulosics, pp. 219-230. *In* G.O. Phillips and P.A. Williams, eds. **Handbook of Hydrocolloids**. Woodhead Publishing Limited, Cambridge.
- Nisperos-Carriedo, M.O. 1994. Edible coatings and films based on polysaccharides, pp. 305-335. *In* J.M. Krochta, E.A. Baldwin and M.O. Nisperos-Carriedo, eds. **Edible Coatings and Films to Improve Food Quality**. Technomic Publishing Company, Inc., Pennsylvania.
- Onsøyen, E. 1992. Alginate, pp. 1-24. *In* A. Imeson, ed. **Thickening and Gelling Agents for Food**. Blackie Academic & Professional, London.
- Pinthus, E.J., R.P. Singh, I.S. Saguy and J. Fan. 1998. Formation of resistant starch during deep-fat frying and its role in modifying mechanical properties of fried patties containing corn, rice, wheat, or potato starch and water. **J. Food Process Pres.** 22: 283-301.
- Rajkumar, V., R. Moreira and M. Barrufet. 2003. Modeling the structural changes of tortilla chips during frying. **J. Food Eng.** 60: 167-175.
- Rapaille, A. and J. van Hemelrijck. 1992. Modified starches, pp. 171-201. *In* A. Imeson, ed. **Thickening and Gelling Agents for Food**. Blackie Academic & Professional, London.
- Sanchez, C. and P. Paquin. 1997. Protein and protein-polysaccharide microparticles, pp. 503-528. *In* S. Damodaran and A. Paraf, eds. **Food Proteins and Their Applications**. Marcel Dekker, Inc., New York.
- Shih, F.F. 2004. Rice proteins, pp. 143-162. *In* E.T. Champagne, ed. **Rice: Chemistry and Technology**. American Association of Cereal Chemists, Inc., Minnesota.

- Sime, W.J. 1990. Alginates, pp. 53-78. *In* P. Harris, ed. **Food Gels**. Elsevier Science Publishers Ltd., London.
- Trudso, J.E. 1991. Hydrocolloids, pp. 223-235. *In* J. Smith, ed. **Food Additive User's Handbook**. Blackie and Son Ltd., London.
- Whistler, R.L. and J.N. BeMiller. 1999. **Carbohydrate Chemistry for Food Scientists**. American Association of Cereal Chemists, Inc., Minnesota.
- Whitaker, J.R. 1972. **Principles of Enzymology for the Food Sciences**. 1st ed. Marcel Dekker, Inc., New York.
- Williams, P.A. and G.O. Phillips. 2000. Introduction to food hydrocolloids, pp. 1-19. *In* G.O. Phillips and P.A. Williams, eds. **Handbook of Hydrocolloids**. Woodhead Publishing Limited, Cambridge.
- Yamsaengsung, R. and R.G. Moriera. 2002. Modeling the transport phenomena and structural changes during deep fat frying; Part I: model development. **J. Food Eng.** 53: 1-10.
- Zecher, D and R. van Coillie. 1992. Cellulose derivatives, pp. 40-65. *In* A. Imeson, ed. **Thickening and Gelling Agents for Food**. Blackie Academic & Professional, London.

APPENDICES

Appendix A
Analytical methods

ANALYTICAL METHODS

1. Moisture content (AOAC, 1995) (Method 925.10)

1.1 Apparatus

1.1.1 Weight balance

1.1.2 Hot air oven

1.1.3 Moisture can

1.1.4 Desiccator

1.2 Procedure

A well-ground sample is weighed accurately 2 g in cooled and weighed moisture can, previously heated to $130 \pm 3^{\circ}\text{C}$ until weight is constant. Uncover sample and place it in the hot air oven. Moisture can, cover and sample are dried in the hot air oven at $130 \pm 3^{\circ}\text{C}$ for 1 hr after oven recovers its temperature. Cover moisture can while still in the hot air oven and transfer to a desiccator as quickly as possible. Weigh moisture can after it reach room temperature, usually 40-60 min, and follow this procedure until weight is constant. Weight loss is determined as moisture content.

1.3 Calculation

Calculated % moisture content by this equation:

$$\% \text{ Moisture content} = \frac{A}{B} \times 100$$

A = Moisture loss of sample in grams

B = Original weight of sample in grams

2. Protein content (BÜCHI manual)

2.1 Apparatus

2.1.1 Weight balance

2.2.2 Kjeldahl flasks

2.2.3 Digestion unit (BÜCHI, model K-435, BÜCHI Labortechnik AG, Flawil, Switzerland)

2.2.4 Scrubber (BÜCHI, model B-414, BÜCHI Labortechnik AG, Flawil, Switzerland)

2.2.5 Distillation unit (BÜCHI, model B-324, BÜCHI Labortechnik AG, Flawil, Switzerland)

2.2.6 Erlenmayer flask

2.2.7 Buret

2.2 Chemical reagent

2.2.1 2 % Boric acid

2.2.2 Concentrated sulfuric acid

2.2.3 Copper sulfate

2.2.4 Ethanol

2.2.5 Mixed indicator (bromocresol green and methyl red)

2.2.6 Potassium sulfate

2.2.7 35 % Sodium hydroxide

2.2.8 0.1 N Sulfuric acid

2.2.9 Tris buffer

2.3 Procedure

2.3.1 Weigh accurately 1 g of finely ground sample and put into digestion flask. Add catalyst, including 10 g of potassium sulfate and 0.5 g of copper sulfate, and 2-3 glass beads. Then, digestion flask with sample and catalyst is added with 20 ml of concentrated sulfuric acid. Digest until solution is clear and then is removed and cooled, but does not allow crystallization.

2.3.2 Connect digestion flask to distillation unit and add 60 ml of distilled water. Gently add 50 ml of 35 % of sodium hydroxide until solution turns brown.

2.3.3 Place erlenmeyer flask containing 60 ml of 2 % boric acid-mix indicator (bromocresol green and methyl red, which are dissolved in ethanol) solution under condenser tube with tip of condenser tube immersed under surface of solution.

2.3.4 Titrate distillate to neutrality with standard 0.1 N sulfuric acid until gray-brown color (end-point) is appear, using buret graduated in 0.1 ml. Read ml of used acid, directly from buret in sample minus blank, all ingredients except sample.

2.3.5 Factor of acid for titration is determined. Weigh accurately 120 mg of tris buffer and dissolve into 200 ml of distilled water. Drop 2-3 of bromocresol green and titrate with acid until gray-brown color is appearing. Read ml of used acid.

2.4 Calculation

Calculated % nitrogen and % protein content by these equations:

$$\% \text{ Nitrogen} = \frac{(S-B) \times N \times f \times 1400}{W}$$

$$\% \text{ Protein content} = \% \text{ Nitrogen} \times 5.95$$

S = Volume of acid consumption for titration sample in ml

B = Volume of acid consumption for titration blank in ml

N = Normality of acid

f = Factor of acid for titration (prepared by following equation)

W = Sample weight in mg

Where factor for rice = 5.95

Calculated factor of acid for titration by this equation:

$$f = \frac{E}{121.14 \times N \times V}$$

N = Normality of acid

V = Volume of acid consumption for titration in ml

E = Tris buffer weight in mg

3. Lipid content (Tecator manual)

3.1 Apparatus

3.1.1 Extraction unit (Tecator, model Soxtec system HT 1043, Tecator AB, Höganäs, Sweden)

3.1.2 Service unit (Tecator, model Soxtec system HT 1046, Tecator AB, Höganäs, Sweden)

3.1.3 Filter paper (No.1)

3.1.4 Thimble

3.1.5 Extraction cup

3.1.6 Hot air oven

3.1.7 Weight balance

3.1.8 Desiccator

3.2 Chemical reagent

3.2.1 Petroleum ether

3.3 Procedure

3.3.1 Weigh 2 g of well-mixed sample (W_1) in filter paper and put into thimble.

3.3.2 Add 50 ml of petroleum ether into extraction cup (W_2), previously heated to 100 °C.

3.3.3 Transfer thimble and extraction cup to extraction unit.

3.3.4 Extract with petroleum ether by boiling for 15 min and rinsing for 45-60 min, and then evaporated petroleum ether.

3.3.5 Place extraction cup in hot air oven at 100°C for 1 hr, cool to room temperature in desiccator and weigh (W_3).

3.4 Calculation

Calculated % lipid content by this equation:

$$\% \text{ Lipid content} = \frac{W_3 - W_2}{W_1} \times 100$$

W_1 = Weight of sample in grams

W_2 = Weight of extraction cup in grams

W_3 = Weight of extraction cup and sample lipid in grams

4. Ash content (AOAC, 1995) (Method 923.03)

4.1 Apparatus

4.1.1 Porcelain crucible

4.1.2 Bunsen burner

4.1.3 Muffle furnace

4.1.4 Weight balance

4.1.5 Desiccator

4.2 Procedure

4.2.1 Weigh 3-5 g of well-mixed sample into porcelain crucible that previously ignited with muffle furnace, cool in desiccator, and weigh soon after attaining room temperature.

4.2.2 Burn sample in porcelain crucible with bunsen burner until fumeless.

4.2.3 Place in muffle furnace at 550°C. Incinerate until light gray is obtained or weight is constant. Ash must not be allowed to fuse. Cool in desiccator and weigh soon after it reaches room temperature.

4.3 Calculation

Calculated % ash content by this equation:

$$\% \text{ Ash content} = \frac{W_2 - W}{W_1 - W} \times 100$$

W = Weight of porcelain crucible in grams

W₁ = Weight of porcelain crucible and sample before incineration in grams

W₂ = Weight of porcelain crucible and sample after incineration in grams

5. Amylose determination (Modified from Chrastil, 1987)

5.1 Apparatus

5.1.1 Weight balance

5.1.2 Vortex mixer

5.1.3 Water bath

5.1.4 Centrifuge

5.1.5 Spectrophotometer

5.2 Chemical reagent

5.2.1 85 % Methanol

5.2.2 0.4 and 0.13 N Sodium hydroxide

5.2.3 0.5 % Trichloroacetic acid

5.2.4 0.01 N Iodine-Potassium iodide solution (1.27 g of iodine per L and 3 g of potassium iodide per L)

5.2.5 Potato amylose

5.3 Procedure

5.3.1 Standardization and measurement

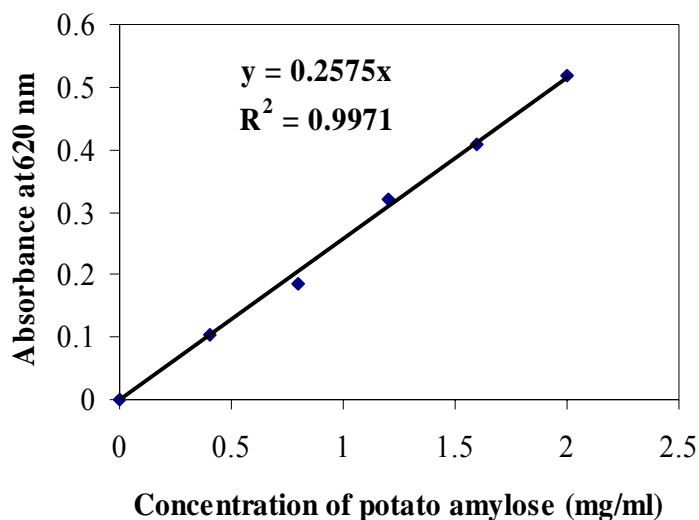
Potato amylose (50 mg) is solubilized with 8.3 ml of 0.4 N sodium hydroxide. Adjust volume to 25 ml with distilled water and heat at 95°C for 30 min in water bath to produce stock solution. Adjust stock solution with 0.13 N sodium hydroxide to produce 0, 20, 40, 60, 80 and 100 % concentration of standard solution. Add 0.1 ml of standard solution into 5 ml of 0.5 % trichloroacetic acid, mix thoroughly, and then mix immediately with 0.05 ml of 0.01 N iodine-potassium iodide solution. Read absorbance of standard solution at 620 nm, used blank (0.13 N sodium hydroxide) to set zero spectrophotometer. Standard curve is produced by plot absorbance at 620 nm against amylose concentration (mg/ml) of standard solution.

5.3.2 Sample preparation and measurement

Mix 10-20 mg of flour with 5 ml of 85% methanol and heat at 60°C for 15 min. Centrifuge sample at 3000 g for 15 min, discard supernatant liquor and collect solid. This process is repeated for 2 times to remove lipids in sample. Solubilize lipid-free sample with 2 ml of 0.4 N sodium hydroxide and add 4 ml of distilled water, and then heat at 95°C for 30 min. Add 0.1 ml of solubilized solution into 5 ml of 0.5 % trichloroacetic acid, mix thoroughly, and then mix immediately with 0.05 ml of 0.01 N iodine-potassium iodide solution. Read absorbance of sample at 620 nm, used blank (0.13 N sodium hydroxide) to set zero spectrophotometer. Use absorbance values obtained from sample, read their amylose content to nearest first decimal place from the standard curve.

5.4 Calculation

Calculated % amylose content by using the standard curve of potato amylose in mg/ml of solution:



Appendix Figure A1 Standard curve of potato amylose for amylose determination.

6. Pasting properties (Newport Scientific manual)

6.1 Apparatus

6.1.1 Weight balance

6.1.2 Rapid visco analyzer (RVA)

6.1.3 Refrigerate circulate bath (NESLAB, model RTE-221, NESLAB Instruments, Inc., Newington, USA)

6.1.4 Canister

6.1.5 Paddle

6.2 Chemical reagent

6.2.1 Distilled water

6.3 Procedure

6.3.1 Weigh 3 g of flour (12% moisture basis) and transfer onto water surface in canister, previously added 25 ml of water. Equivalent sample and water mass are calculated by using below equations.

6.3.2 Place paddle into canister and vigorously jog blade up and down through sample for 10 times. If any flour lumps remain on water surface or adhere to paddle, repeat jogging action.

6.3.3 Place paddle into canister, and insert paddle and canister assembly firmly into paddle coupling so that paddle is properly centered. Initiate measurement cycle by depressing motor tower of instrument. Do not allow flour to stand in the water for more than 1 min before started test. Test proceeds and ends automatically as followed:

Time	Type	Value
00:00:00	Temperature	50°C
00:00:00	Speed	960 rpm
00:00:10	Speed	160 rpm
00:01:00	Temperature	50°C
00:04:45	Temperature	95°C
00:07:15	Temperature	95°C
00:11:06	Temperature	50°C

End of test; 00:12:30

6.4 Calculation

Equivalent sample and water mass are calculated by these equations:

$$S = \frac{88 \times 3}{100 - M} \quad \text{for flour}$$

$$W = 25 + (3 - S) \quad \text{for water}$$

S = Corrected sample weight in grams

W = Corrected water weight in grams

M = Actual moisture content of sample

Appendix B
Statistical Analysis

Appendix Table B1 Statistical analysis of composition of rice flour and waxy rice flour.

Treatment	Source	Degree of Freedom (df)	Type III Sum of Squares (SS)	Mean Squares (MS)	F	Sig.
Moisture	Treatment	3	1.828	0.609	1.475	0.293
	Error	8	3.305	0.413		
	Total	11	5.134			
Protein	Treatment	3	31.779	10.593	1162.452	0.000
	Error	4	0.036	0.009		
	Total	7	31.815			
Lipid	Treatment	3	0.114	0.038	21.048	0.000
	Error	8	0.014	0.002		
	Total	11	0.129			
Ash	Treatment	3	0.044	0.015	237.624	0.000
	Error	8	0.000	0.000		
	Total	11	0.045			

Appendix Table B2 Statistical analysis of RVA pasting profiles of rice flour and waxy rice flour containing different protein contents.

Treatment	Source	Degree of Freedom (df)	Type III Sum of Squares (SS)	Mean Squares (MS)	F	Sig.
Pasting temperature	Treatment	3	11.968	3.989	1.163	0.427
	Error	4	13.722	3.431		
	Total	7	25.690			
Peak time	Treatment	3	14.541	4.847	8616.970	0.000
	Error	4	0.002	0.001		
	Total	7	14.543			
Peak viscosity	Treatment	3	3095226.000	1031742.125	293.599	0.000
	Error	4	14056.500	3514.125		
	Total	7	3109283.000			
Holding strength	Treatment	3	560832.600	186944.198	80.840	0.000
	Error	4	9250.125	2312.531		
	Total	7	570082.700			
Final viscosity	Treatment	3	11000000.000	3504598.333	827.508	0.000
	Error	4	16940.500	4235.125		
	Total	7	11000000.000			

Appendix Table B3 Statistical analysis of amylose content of rice flour and waxy rice flour.

Source	Treatment	df	SD	MD	t-test	Sig. (2-tailed)	95% confidence Interval of Difference	
							Lower	Upper
Equal variances assumed	Amylose content	2	1.161	25.624	22.080	0.002	20.631	30.618

Appendix Table B4 Statistical analysis of effect of protein content of rice flour and waxy rice flour on water content, oil absorption and expansion in rice crackers.

Treatment	Source	Degree of Freedom (df)	Type III Sum of Squares (SS)	Mean Squares (MS)	F	Sig.
Moisture content of rice sheet before frying	Treatment	3	0.347	0.116	0.045	0.986
	Error	4	10.409	2.602		
	Total	7	10.757			
Moisture content of rice cracker after frying	Treatment	3	3.887	1.296	1.101	0.446
	Error	4	4.707	1.177		
	Total	7	8.594			
Oil content of rice cracker after frying	Treatment	3	364.871	121.624	1.378	0.370
	Error	4	353.049	88.262		
	Total	7	717.920			
Expansion of width	Treatment	3	435.073	145.024	0.824	0.545
	Error	4	703.852	175.963		
	Total	7	1138.925			
Expansion of thickness	Treatment	3	3122.385	1040.795	5.998	0.058
	Error	4	694.047	173.512		
	Total	7	3816.432			

Appendix Table B5 Statistical analysis of effect of rice flour to waxy rice flour ratios on RVA pasting characteristics in flour composites.

Source	Treatment	df	SD	MD	t-test	Sig. (2-tailed)	95% confidence Interval of Difference	
							Lower	Upper
Equal variances assumed	Pasting temperature	2	0.069	-0.025	-0.360	0.753	-0.324	0.274
	Peak time	2	0.030	0.130	4.333	0.049	0.001	0.259
	Peak viscosity	2	61.690	-370.000	-5.998	0.027	-635.430	-104.570
	Holding strength	2	75.858	-292.500	-3.856	0.061	-618.892	-33.892
	Final viscosity	2	31.325	468.000	14.940	0.004	333.220	602.780

Appendix Table B6 Statistical analysis of effect of rice flour to waxy rice flour ratios and hydrocolloid addition on water content, oil absorption and expansion in rice crackers (factorial analysis).

Treatment	Source	Degree of Freedom (df)	Type III Sum of Squares (SS)	Mean Squares (MS)	F	Sig.
Moisture content of rice sheet before frying	Ratio	3	5.350	1.783	0.544	0.662
	Solution	2	4.260	2.130	0.649	0.541
	Ratio*Solution	6	0.286	0.048	0.015	1.000
	Error	11	36.078	3.280		
	Total	23	60.670			
Moisture content of rice cracker after frying	Ratio	3	1.803	0.601	4.127	0.035
	Solution	2	1.823	0.911	6.259	0.015
	Ratio*Solution	6	0.801	0.134	0.917	0.518
	Error	11	1.602	0.146		
	Total	23	6.062			
Oil content of rice cracker after frying	Ratio	3	441.578	147.193	6.034	0.011
	Solution	2	19.626	9.813	0.402	0.678
	Ratio*Solution	6	105.826	17.638	0.723	0.640
	Error	11	268.326	24.393		
	Total	23	841.178			
Expansion of width	Ratio	3	1975.798	658.599	13.270	0.001
	Solution	2	39.447	19.724	0.397	0.681
	Ratio*Solution	6	119.733	19.955	0.402	0.863
	Error	11	545.948	49.632		
	Total	23	2858.659			
Expansion of thickness	Ratio	3	3173.721	1057.907	0.898	0.473
	Solution	2	2106.079	1053.039	0.893	0.437
	Ratio*Solution	6	13240.835	2206.806	1.872	0.174
	Error	11	12964.494	1178.590		
	Total	23	33289.729			

Appendix Table B7 Statistical analysis of effect of rice flour to waxy rice flour ratios and hydrocolloid addition on water content, oil absorption and expansion in rice crackers (ANOVA).

Treatment	Source	Degree of Freedom (df)	Type III Sum of Squares (SS)	Mean Squares (MS)	F	Sig.
Moisture content of rice sheet before frying	Treatment	11	9.896	0.900	0.213	0.992
	Error	12	50.773	4.231		
	Total	23	60.670			
Moisture content of rice cracker after frying	Treatment	11	4.427	0.402	2.953	0.038
	Error	12	1.635	0.136		
	Total	23	6.062			
Oil content of rice cracker after frying	Treatment	11	567.030	51.548	2.256	0.089
	Error	12	274.148	22.846		
	Total	23	841.178			
Expansion of width	Treatment	11	2134.978	194.089	3.218	0.028
	Error	12	723.681	60.307		
	Total	23	2858.659			
Expansion of thickness	Treatment	11	18520.635	1683.694	1.368	0.299
	Error	12	14769.094	1230.758		
	Total	23	33289.729			

Appendix Table B8 Statistical analysis of effect of 1 % (w/v) hydrocolloid coating on water content, oil absorption and expansion in rice crackers (RF:WF ratio = 0.7:0.3).

Treatment	Source	Degree of Freedom (df)	Type III Sum of Squares (SS)	Mean Squares (MS)	F	Sig.
Moisture content of rice sheet before frying	Treatment	2	0.610	0.305	3.417	0.168
	Error	3	0.268	0.089		
	Total	5	0.878			
Moisture content of rice cracker after frying	Treatment	2	1.022	0.511	1.237	0.406
	Error	3	1.239	0.413		
	Total	5	2.261			
Oil content of rice cracker after frying	Treatment	2	338.207	169.103	6.723	0.078
	Error	3	75.460	25.153		
	Total	5	413.667			
Expansion of width	Treatment	2	905.423	452.711	7.289	0.071
	Error	3	186.337	62.112		
	Total	5	1091.760			
Expansion of thickness	Treatment	2	1547.220	773.610	2.574	0.223
	Error	3	901.777	300.592		
	Total	5	2448.997			

CIRRICULUM VITAE

NAME : Miss Sasikarn Kithikorn

BIRTH DATE : September 11, 1982

BIRTH PLACE : Bangkok, Thailand

EDUCATION	: <u>YEAR</u>	<u>INSTITUTE</u>	<u>DEGREE/DIPLOMA</u>
	2005	KMITNB	B.Sc. (Agro-Industrial Technology)

POSITION/TITLE : -

WORK PLACE : -

SCHOLARSHIP/AWARDS : -